Journal of Pharmaceutical Investigation
https://doi.org/10.1007/s40005-024-00676-9

ORIGINAL ARTICLE

Development and in vitro/in vivo evaluation of a nanosponge formulation loaded with *Boswellia carterii* oil extracts for the enhanced anti-inflammatory activity for the management of respiratory allergies

Sally Abou Taleb[1] · Bassant M. M. Ibrahim[2] · Mona A. Mohammed[3] · Noha Nazeeh Yassen[4] · Alyaa Farouk Hessin[2] · Shaimaa Ali Gad[2] · Asmaa Badawy Darwish[1]

Received: 8 November 2023 / Accepted: 20 February 2024

Abstract

Purpose In several nations, it has been known that *Boswellia carterii* (BC) plants have a long history of usage as an anti-inflammatory medicine. Our current study deals with the study of two different ways of extraction of BC volatile oil and fixed oil as main constituents (Octyl acetate, 46.46% and β-Boswellic acid, 10.21%, respectively), preparation, and evaluation of Nano sponges loaded with either dexamethasone (DEX) or *B. carterii* volatile/fixed oil mixture.

Methods Nano sponges were created utilizing an ultrasound-assisted synthesis method. Using spectrophotometry, the entrapment efficiency (EE%) of drugs in Nano sponges was considered. Several techniques were used to characterize Nano sponges.

Results EE% of drugs inside Nano sponges ranged from 99.15 ± 3.50 to 100% ± 4.76%. Particle size of Nano sponges ranged from 59.9 ± 26.3 to 229.2 ± 30.23 nm. Drugs released from Nano sponges bi-phasically according to Korsmeyer–Peppas model. The anti-inflammatory activity of either *B. carterii* oil mixture or Dexa salt and their Nano formulations (D4 and O1) in the treatment of respiratory allergy were evaluated in rat model mimicking chronic allergic respiratory diseases. Histopathologic examinations and measurement of Intracellular adhesion molecule-1 (ICAM-1), Leukotriene B_4 (LTB_4) and Interleukin β4 (ILβ4) levels exposed that, the treatment significantly lowered the levels of the inflammatory biomarkers in treated rats and exhibited improved histopathologic profiles when compared to positive control group.

Conclusion *Boswellia* oil and its Nano sponge formulation O1 as well as Dexa salt Nano sponge formulation D4 had promising therapeutic effects on upper and lower respiratory allergic conditions.

Keywords *Boswellia carterii* · Volatile/fixed oil · Inflammatory · Allergy · Nano sponges · Drug delivery

Introduction

Traditional herbal medicine practitioners have detailed the therapeutic usefulness of several indigenous plants for various ailments. Indigenous plants are still used as a primary health care system in different parts of the world, where local empirical knowledge about plant medicinal characteristics serves as the foundation for their usage as a home medicine and continues to bring novel treatments to humans. Advances in separation and characterization technology have offered practical tools to the active constituents of medicinal plants and specifically identified the biologically active compounds, which rendered the use of whole plants as a drug to treat particular diseases unacceptable. Metabolomics is the most recent and well-integrated specialty that contributes to this field. Metabolomics has

✉ Mona A. Mohammed
monaarafamohammed@yahoo.com

✉ Asmaa Badawy Darwish
dr-asmaaa@hotmail.com

[1] Pharmaceutical Technology Department, National Research Centre, 33 El-Buhouth Street, Dokki, Giza 12622, Egypt

[2] Pharmacology Department, Medical and Clinical Studies Research Institute, National Research Centre, Dokki, Giza 12622, Egypt

[3] Medicinal and Aromatic Plants Research Department, Pharmaceutical and Drug Industries Research Institute, National Research Centre, Giza, Egypt

[4] Pathology Department, Medical and Clinical Studies Research Institute, National Research Centre, Dokki, Giza 12622, Egypt

Published online: 08 April 2024

rapidly progressed and significantly impacted both fundamental and applied sciences (Oliver et al. 1998).

The prevalence of atopic disorders (AD) such as asthma, allergic rhinitis, atopic dermatitis, and food allergy has steadily increased over the previous 10 years, with the highest incidence for asthma, followed by allergic rhinitis. Atopic dermatitis, and food allergy, respectively, affects about 15–20% of children and a population of about 2–10% of adults (Capozza et al. 2023). Impaired immune system function and persistent inflammation increase vulnerability to repeated respiratory infections. AD represents a health burden to patients due to the high treatment costs besides the inability to perform daily regular work (Allenova and Darlenski 2023). Until now, AD treatments target inflammation using local-acting corticosteroids and systemic immunosuppressive medications (Tham and Leung 2019).

Dexamethasone (DEX) is regarded as a potent corticosteroid widely used to treat inflammations caused by several diseases. DEX has proven its efficiency in managing postoperative inflammations, notably when other therapeutic agents have failed to provide treatment benefits. However, the use of DEX has many drawbacks, such as a short half-life that requires repetitive administration of the drug and multiple side effects with prolonged use like hypertension, hydro electrolytic disorders, hyperglycaemia, peptic ulcers, and glucosuria; this limits the use of dexamethasone in long-term treatment (Schimmer and Parker 1996).

As a potentially safer alternative to topical terpenes, tripenes and steroids from natural products (Mohammed 2023) such as *Boswellia carterii i* volatile and fixed oils can be used in cases of inflammation associated with allergy due to their anti-inflammatory effects (Borotová et al. 2023). Trees in the Boswellia genus are prized for their fragrant resin, which has several medicinal uses, most notably as anti-inflammatory drugs. Components of the resin called boswellic acids have showed promise in the management of inflammatory disorders, such as asthma (Yassin et al. 2013).

For a long time, the development of new systems has required sophisticated chemistry, which has mainly thwarted efforts to create effective targeted mechanisms for delivering drugs. The development of the Nanocomposite Spongey delivery system for drugs has shown to be a big step in the right direction. Nano sponges (NSs) are a novel method for medicine administration. They are nanoscale sponge-like structures with several chambers capable of holding drugs. NSs are colloid structures made of polymers that are highly cross-linked being capable of distributing payloads owing to its porous exterior surfaces. Lipophilic and hydrophilic pharmaceuticals can be held in these polymeric sponge-like structures, enhancing the aqueous solubility and bioavailability of poorly soluble medicines (Girigoswami and Girigoswami 2022).

Because of their distinctive three-dimensional network and functional groups, NSs based on cyclodextrin are currently widely employed in the pharmaceutical sector to interact with biological tissues and promote bio adhesion. The targeted location can be reached by these small sponges passing through the body; once there, they adhere to the surface and begin releasing drugs gradually and accurately. Since the drug may be released at the precise target site rather than dispersing throughout the body, it will be more effective for a given dosage. Another significant feature of these sponges is their aqueous solubility, which enables successful application of these systems for medications with low solubility (Utzeri et al. 2022).

This work aims to fabricate a locally acting nano-composite delivery system loaded with DEX or BC oil mixture. The new system can be used to alleviate signs and symptoms of allergic rhinitis that occur as a part of AD in an attempt to prevent progression to bronchial asthma. Nano-composite delivery systems can enhance the efficacy of loaded drugs, avoiding severe side effects accompanied by oral administration, such as hepatic first-pass metabolism, gastric irritation, and compliance problems, and providing better treatment convenience.

Materials and methods

Materials

Boswellia carterii resins collected from Khartoum; Sudan governorate, this collection complies with local and national guidelines as permission was obtained for collection of plant material. Dexamethasone Sodium Phosphate was a gift from AMRIYA Pharmaceutical Industry Company, Egypt. Hydroxyprobyl β-cyclodextrin (HPβ-CD) (KLEPTOSE HPB, MW 1380) was kindly provided by Roquette (France). Diphenyl carbonate (DPC) was purchased from Acros Organics (Belgium). Prednisolone was purchased from Sigma Chemical Co. (St Louis, MO, U.S.A.). Disodium hydrogen phosphate anhydrous and Potassium dihydrogen phosphate were purchased from El-Gomhouria Pharmaceutical Chemicals (Egypt). Cellulose membrane was purchased from Sigma-Aldrich, chemie Gmbh, Steinheim, Germany. All other chemicals and solvent are of chemical grade and used without further purification. ELISA Kits for determination of allergic and inflammatory markers: Intracellular adhesion molecule 1(ICAM-1), Leukotriene B_4 (LTB_4) and Interleukinβ 4 (ILβ4) levels in serum were purchased from Elabscience Inc (USA).

Animals

Male Wistar albino rats weighing 150–175 g were obtained from the National Research Centre's animal house colony in Dokki, Giza, Egypt. The rats were housed in common metal cages and kept in an air-conditioned space with a temperature of 22 °C and a humidity of 55°F with unlimited access to water. The current study complies with regional and federal regulations because it was carried out in accordance with the guidance for the care and use of laboratory animals and was granted clearance by the National Research Centre ethics committee under certificate number 19/209. The Institutional Animal Ethical Committee (IAEC) and the National Regulations of Animal Welfare in Egypt were followed when conducting the experiments, and the results were reported in line with Animal Research: In-Vivo Experiment Reporting (ARRIVE).

Methods

Plant extraction, volatile, and fixed oils from BC gum resin

Fixed and volatile oils are extracted substances from resin. The present study was carried out on *Boswellia carterii* resins collected from Khartoum; Sudan governorate. It was identified by Dr. Gibali, M.A. Department of Taxonomy, and Faculty of Science Cairo University then the estimation of volatile and fixed oil content (Rhimi et al. 2022). (i) The volatile oil of 50 g dry resins sample was extracted by the water distillation method (4 h) in a Clevenger's apparatus (Guenther 1952). The resulted volatile oil of each treatment was separately dehydrated with anhydrous sodium sulphate and kept in the deep freezer until GC/MS analysis (Hamed et al. 2019). Each sample was done in triplicate and the mean values of the oil content (%) were recorded as 5.2 ± 0.8 ml. (ii) 355 g of air-dried fine powder of (BC) fruits were extracted by petroleum ether 40–60 °C using Soxhlet apparatus till complete extraction given 152 g. The extract was evaporated by rotary evaporator at 40 °C till dry, and then the residue was kept in vacuum desiccators till constant weight and total lipid content was calculated to be 42.25% (Rhimi et al. 2022).

Separating and classifying saponifiable and non-saponifiable substances

Two ml fixed oil was saponified (KOH) and determined (Kinsella 1966). The amount of fatty acid methyl esters was measured using GC/MS in the Chromatography unit at Bani Suef University, and it was used to establish a profiling list of fatty acid methyl ester metabolites (Mohammed et al. 2016). By contrasting the respective retention durations of the separated compounds with those of readily available reference compounds injected under the same circumstances, it was possible to identify the methyl esters of fatty acids, sterols, and hydrocarbon compounds. The area of the observed peak region served as the basis for the quantitative determination of each chemical (Mohammed et al. 2021).

Chromatographic procedure

Gas chromatography–mass spectrometry analysis (GC–MS) Analyses were conducted using the GC–MS (Agilent Apparatus) at the Central Laboratories Network, National Research Centre, Cairo, Egypt. The equipment includes a gas chromatograph (7890B) and mass spectrometer detector (5977A). The GC was outfitted with an HP-5MS column that measured 30 m and had an internal diameter and film thickness of 0.25 mm. He was used as the carrier gas, with data being collected at the following temperature programmed and flow rates of 1.2 ml/min at a split of 1:30: 45 °C for 4 min; 4 °C/min increase to 150 °C and hold for 8 min; 6 °C/min increase to 210 °C and hold for 1 h. At 280 °C and 220 °C, respectively, the injector and detector were maintained by employing a spectral range of m/z 50–900 and a solvent delay of 5 min, mass spectra were produced by electron ionization (EI) at a power of 70 eV. By contrasting the spectrum fragmentation pattern with those found in the Wiley and NIST Mass Spectral Library data, many constituents were identified (Mohammed et al. 2022a, b).

UPLC-HRMS (lipidomic technique) of oils BC resins One ml of methanol was added to 100 ul of oil from dried *B. carterii* resins extracted with petroleum ether. The extract was filtered before being mixed with a Q-Exactive hybrid MS/MS quadrupole—Orbitrap mass spectrometer (Thermo, Bremen, Germany) in negative ion mode. For the chromatographic separation of this system, deionized water acidified with 0.1 percent formic acid (solvent A) and acetonitrile (solvent B) were utilized, together with the BEH shield C18 column (1502.1 mm, 1.7 m). The mobile phase flow was changed to the following gradient for the duration of 5 min: (0–14 min) from 5 B to 50% B, (14–20 min) to 98 percent B. The system was then returned to its default settings and given three minutes to re-adjust. The Q-Exactive MS was operated at the following settings: the HESI ion source voltage (− 3 kV or 3 kV). The flow rate of the gas (N2) is 48 l/min, while the flow rate of the auxiliary gas is 13 l/min. The temperature of the auxiliary gas heater is 380 °C, whereas the ion source capillary is 250 °C. The CID MS/MS investigations' collision energy was 15 eV (Mohammed et al. 2021).

Data processing

To give a thorough fragmentation pattern with retention time and MSMS information, mass spectral fragmentations of 50 metabolites were carried out using ion mobility tandem mass spectrometry (MSMS). The petroleum ether extract oil fractions were packed in MS-DIAL 4.90 (http://prime.psc.riken.jp/), which exported a common output 'Analysis Base File' (ABF) format from raw MS data import. Through the use of (MSP) format libraries to filter noisy spectra using a traditional spectral similarity computation, this resulted in an improved standardized untargeted lipidomic. By comparing the fragmentation patterns and retention indices (RI) of the chosen probable metabolites with those found in the KNApSAcK, Metlin, Golm, MassBank, Fiehn Bin Base, LipidBlast, ReSpect, and RIKEN databases, the metabolites were found and identified (Ammar et al. 2021; Mohammed et al. 2022a, b).

Preparation of nano sponges

A modified version of the ultrasound-assisted synthesis approach was employed to create NSs. Distilled water combined a specified molar ratio of diphenyl carbonate (DPC), a cross-linker, and hydroxypropyl cyclodextrin (HPβ-CD), a polymer. The ratios employed were 1:1, 1:3, 1:4, and 1:6 (HPβ-CD: DPC) (Table 5). The mixture was sonicated at 90 °C (Trotta et al. 2008; Abou Taleb et al. 2019), then homogenized in a hot water bath for 7 min at 12,000 rpm. The liquid was poured into falcon tubes and centrifuged for 30 min at 6000 rpm. After centrifugation, the drug was added, and the mixture was shaken at 150 rpm for the remainder of the night. The solution was centrifuged for 30 min at room temperature after being sonicated at 90 °C in the following day. The mixture was put into a petri dish, and the volume was adjusted for freeze-drying. It was then kept at 25 °C until it was used again. (Ansari et al. 2011b; Selvamuthukumar et al. 2012). The resulting Nano sponges will be uniformly sized and spherical in shape.

Determination of loading efficiency of NSs

NSs containing a precisely weighed quantity (10 mg) of DEX salt were stirred continuously in a 100 ml buffer solution (pH 7.4) for 50 min. Samples were filtered using a 0.22 m membrane filter before being analyzed with an ultraviolet–visible (UV) spectrophotometer (Pharma spec 1700, Shimadzu, Japan) at the preset λ_{max}, at 242 nm (Al-Owaidi et al. 2021) The following equation was used to calculate encapsulation efficiency for all ratios:

$$EE\% = \left(M_{act}/M_{the}\right) \times 100$$

where M_{act} is the actual DEX content in the weighed quantity of Nano sponges, and M_{the} is the theoretical DEX content in Nano sponges (Kılıçarslan and Baykara 2003; Ahmed et al. 2021).

Vesicle size, polydispersity index and zeta potential measurement

The prepared formulations' vesicle size, polydispersity index, and Zeta Potential were measured by the Zeta-sizer (Malvern Zeta-sizer Nano ZS, Malvern Instruments, UK) using dynamic light scattering (DLS), a method based on laser diffraction, at room temperature. At a scattering angle of 90.0°, the intensity of the scattered light's time-dependent correlation function was measured (Abou Taleb et al. 2022).

Optimization of the selected NSs formulation

Following the completion of the tests, as mentioned earlier, the best molar ratio between HPβ-CD and DPC was selected to be the optimized ratio to prepare DEX salt NSs with the optimum EE%, PS and ZP values (D4). The same molar ratio HPβ-CD: DPC (1:6), was used for the preparation of BC mixed oils (1:1) extract NSs (O1). The new oil formulation was prepared as the same method previously mentioned in "Preparation of Nano sponges" section.

Determination of EE%, PS, ZP and PDI of Oil Ns formulation

The EE% of the prepared oil formulation was measured at the predetermined $\lambda_{max,}$ at 233 nm as previously mentioned in "Determination of loading efficiency of NSs" section. The composition, encapsulation efficiency and physico-chemical properties of the optimized formulations are presented in Table 5.

Characterization of the optimized formulations

Surface morphology Transmission electron microscopy (TEM)

Using TEM (JEOL Co., JEM-2100, Japan), the morphological properties of DEX and Oil NSs were investigated. A copper grid that had been coated with carbon was given one drop of the diluted sample, and the grid was allowed to dry for 15 min at room temperature before the samples were stained. The grid was coated with a tiny amount of phosphotungstic acid solution (1%w/v), let to stand for three minutes, and then put into the microscope, where samples were inspected for surface features and shape at various magnifications (Swaminathan et al. 2010).

Scanning electron microscopy (SEM)

SEM (Quanta FEG 250, ThermoFisher Scientific Co., Czech Republic) was used to examine the surfaces of the optimized formulations. Freeze-dried samples were double-sided taped on aluminum stubs before being sputter-coated a thin coating of gold. At a distance of 10 mm and an acceleration voltage of 20 kV, SEM was employed (Abou Taleb et al. 2022).

X-ray powder diffraction To examine the impact of inclusion complex phenomena on the drug's crystallinity, the XRD spectra of DEX and oil NSs, as well as individual components such HP-CD, DPC DEX salt, and oil extract, were taken using a high-power powder X-ray diffractometer (Seimens, Model D5000, German). Quartz was used as the calibration internal standard. Powdered samples were subjected to Ni-filtered (Cu-k) radiation given at a 45 kV voltage and 40 mA current. Between 4 and 50 degrees, samples were examined. The recording employed a 2 o/min scanning speed with a 0.02 o step size. Calculated was the crystallinity's % (Shankar and Agrawal 2015).

Fourier transform infrared spectroscopy analysis To find out if there were any possible drug interactions with the components of the selected NS formulations, Fourier transform infrared spectroscopy (FT-IR) analysis using the KBr pellet method and an FT-IR spectrophotometer (JASCO 6100, Tokyo, Japan) was utilized.

In-vitro release study

This study employed free DEX, oil solutions, and DEX and oil NSs formulations (D4 and O1). The dialysis bags (Dialysis tubing cellulose membrane, Sigma-Aldrich Co., St. Louis, USA; Molecular weight cut-off 12,000–14,000) were filled with amounts equal to 2 mg of the NSs formulations, DEX, and oil aqueous solutions, and the cut-off value for molecular weight was 12,000–14,000. Before being put into 100 ml screw-capped glass containers filled with 100 ml PBS pH 7.4 to preserve sink condition, the bags were sealed on both sides to prevent leaking. The experiment was conducted in a thermostatic shaking water bath (Memmert, SV 1422, Germany) at 37 ± 0.5 °C and 100 rpm. Regular sample replacement with a similar amount of replacement release medium was done to maintain the sink condition. The DEX and oil concentrations were determined by spectrophotometric analysis and compared to blanks that had undergone the same treatment. The cumulative release percentages were calculated by dividing the drug release by the medication's initial concentration in the dialysis bag. Each measurement was carried out in triplicate, and three separate samples were used. Numerous mathematical models, including zero, first order, Higuchi's square root of time model, and Krosmeyr Peppa's kinetic models, were used in the kinetic analysis of drug release from NSs formulations (Basha et al. 2015).

Pharmacological study

Experimental design of the efficacy study Male Wistar albino rats were used for the biological evaluation of the formulations' efficacy. Forty-eight rats were divided into 6 groups at random (n = 8). Rats in group I acted as the negative control group and received oral saline solution 0.9%. For the duration of 120 days, Group II was given acetaminophen suspended in yoghurt via oral gavage in order to induce allergic rhinitis (Mohammed et al. 2022a, b) and served as a positive control group. Groups III, IV, V and VI received acetaminophen as group II, then they were treated with a dose of 10 µl equivalent to 20 µg of Free BO extract, Free DEX, DEX NSs and BO NSs, respectively instilled in each rat's nostril (IN) for 28 days.

Preparation of blood samples and biochemical analysis of anti-inflammatory and anti-allergic markers At 24 h following the final therapy dosage, blood samples were taken from all rats' retro-orbital plexus veins. Samples were centrifuged at room temperature for 10 min at 1500 rpm to separate the serum after clotting (Sorg and Buckner 1964). Serum samples were stored at − 20 °C for analysis of intercellular adhesion molecule-1 (ICAM-1), interleukin β 4 (ILβ 4) and Leukotriene B_4 (LTB_4) and levels in serum by using ELISA kits.

Preparation of tissues for Histopathologic examination All groups were sacrificed. Each animal's nose, trachea, and lungs were removed, fixed in 10% neutral formalin solution for 24 h, and then embedded in paraffin. After being rinsed in tap water for 30 min, all specimens were dehydrated in varying amounts of alcohol, cleaned in xylene, and embedded in paraffin. Hematoxylin and eosin were used to stain serial slices each three millimeters thick (Drury and Wallington 1980) to be examined histopathologically. Images were taken at the National Research Centre's pathology lab utilizing an image analysis system with an Olympus CX41 light microscope and an SC100 video camera connected to a computer system. Numerous photomicrographs were captured at various magnifications.

Statistical analysis

Values were given as means ± standard error. One-way analysis of variance (ANOVA) was used to compare means, followed by the Tukey–Kramer multiple comparisons test. In all varieties of statistical tests, $p \leq 0.001$ was considered as being significant. All statistical analyses were performed using GraphPad Prism software, version 8.

Results and discussion

Volatile oil extraction and chromatography of *B. carterii* resins by GC/MS

Trees in the genus *Boswellia* provide the resin used to make essential oils (family Burseraceae). To develop exuded gum, which looks like a milk-like resin, cuts are made in the tree trunks. The resin becomes frankincense, an orange-brown gum resin that has dried. *B. carterii* grows in Sudan, and China, and *B. sacra* grows in Arabia. It has been used by ancient Egyptians, and the aroma of these resins has been esteemed for its putative therapeutic effects and excellent qualities for religious ceremonies (DeCarlo et al. 2020). Numerous health-promoting qualities of frankincense resin have been thought to exist throughout history. Rheumatoid arthritis and other inflammatory disorders have been treated with the resins of the *Boswellia serrata* in many different cultures (Lindler et al. 2020).

In the First way of extraction; Volatile oils extracted from BC resin by steam hydro distillation are given yield 10.4%. According to GC/MS analysis, the recognized constituents of the essential oil are presented in (Table 1 and Fig. 1a). The resins of BC essential oil composed of forty-seven compounds representative of 94.4% of the total oil constituents. The main ingredients of the essential oil identified with GC/MS are *Octyl acetate* (46.46%, peak no. 18) and *3-Carene* (6.37% peak no. 12), and *D-Limonene* (5.25% peak no. 14) and *Farnesyl acetate* (5.05 peak no. 31). The total amounts of the four major compounds in the volatile oils were 63.13 from 94.04% showed in (Table 1 and Fig. 1a). The oxygenated compounds were 66.61% more than non-oxygenated compounds 27.79%. When comparing the yield% with the other different studies that reported that frankincense resin contains 5–11% of essential oil, it was found that there is a similar correlation with the amount extracted by steam distillation (Al Amri et al. 2019; Ayub et al. 2022). We found that the main constituent of volatile oils resins is *Octyl acetate* (46.46%, peak no. 18), which was different from previous study performed by Ni et al., who uncovered that alpha-pinene 78.45% is the main constituent in *B. sacra*, which may be due to study of different species (Ni et al. 2012). In this respect, the results is nearly similar to that obtained by Hussain et al. (2013) and Mikhaeil et al. (2003), who mentioned that the major compounds in *B. carterii* was octyl acetate (13.4–40%) then Limonene, α-pinene, and octanol.

Lipid profiles of *B. carterii* resins by GC/MS chromatography

In the second extraction procedure, the Soxhlet apparatus extracted 355 g of resin fruit with petroleum ether (40–60 °C) as a total lipid extract. Using a rotating evaporator and lowered pressure at 35 °C, the mixed extracts were concentrated (Ayub et al. 2023) and filtered using Whatman No. 54.

Saponification of the fixed oil of BC-resins

The results in Table 2 and TIC in Fig. 1b represented the forty-four fatty acid methyl esters of different BC resins under investigation. MS was used in this investigation for the qualitative and quantitative determination of individual fatty acids. The major five fatty acids were estimated 46.44% from total lipids as follow: β-Boswellic acid (10.21%), Oleic acid (10.05%), 3-O-acetyl-β-boswellic acid (8.98%), Myristic acid (8.89%), and 11-Keto-beta-boswellic acid (8.31%).

Unsaponification of the fixed oil of BC-resins

The unsaponifiable lipid fraction is a potential source of bioactive components such as, acetophenones, triterpenoids, and various hydrocarbons compounds. GC–MS analyses of the unsaponifiable matter of the BC resins are presented in (Table 3 and Fig. 1c). The highest four compounds are recorded as 4′-Methylacetophenone (47.11%), Squalene (20%), Campesterol (10.15%) and D-Limonene (6.41%). The results revealed the presence of various hydrocarbons ranging from C9 to C31, of which Hydrocarbon Resin C9, dodecane C12, Octacosane C28, and Hentriaconta C31 are the most predominant components. Dealing with percentage the unsaponifiable matter represented the percentage of 83.68% for four compounds from the total thirty-three compounds from the unsaponifiable lipid.

Lipidomic profiles of the fixed oil of BC- resins by LC-MSMS

The lipidomic profiles of the 50 substances examined by LC-MSMS of BC were documented in Table 4 and graphically displayed in Fig. 2 (Mohammed et al. 2021).

Molecular network

When molecules are ionized using lipidomics mass spectrometry, they frequently form multiple ion species with distinct fragmentation behavior. MS-DIAL (4.90) is a method for creating molecular networks from these data. Next, molecular spectrum networking data is created using the GNPS web platform for all signals, and Fig. 2 displays a list of compounds (Mohammed et al. 2021).

Preparation of DEX NSs

In the present study, NSs were prepared by ultrasound assisted technique. This method produces NSs with

Table 1 The main chemical constituents of volatile oil *Boswellia Carterri*

Peak no.	RT	Name	MS (M/e)			Area %
			M/Z	No scans	Chemical formula	
1	4.96	α-Thujene	136	381	$C_{10}H_{16}$	0.05
2	5.38	β-Pinene	136	419	$C_{10}H_{16}$	0.01
3	5.55	α-Phellandrene	136	450	$C_{10}H_{16}$	0.10
4	5.72	α -Pinene	136	498	$C_{10}H_{16}$	0.90
5	6.01	Camphene	136	538	$C_{10}H_{16}$	0.08
6	6.68	β-Phellandrene	136	636	$C_{10}H_{16}$	0.15
7	6.76	Cis-Sabinene	136	666	$C_{10}H_{16}$	0.07
8	7.09	β-Myrcene	136	744	$C_{10}H_{16}$	0.36
9	7.41	2-Carene	136	781	$C_{10}H_{16}$	0.06
10	8.11	**γ-Limonene**	136	907	$\mathbf{C_{10}H_{16}}$	2.59
11	8.33	Trans-β-Ocimene	118	945	C_9H_{10}	0.24
12	8.63	3-Carene	136	1004	$\mathbf{C_{10}H_{16}}$	6.37
13	8.93	γ-Terpinene	136	1050	$C_{10}H_{16}$	0.05
14	9.33	**D-Limonene**	136	1159	$\mathbf{C_{10}H_{16}}$	5.25
15	10.10	Linalool	154	1273	$C_{10}H_{18}O$	0.97
16	10.42	Octanol acetate	172	1321	$C_{10}H_{20}O_2$	1.30
17	12.33	(+)-4-Terpineol	154	1644	$C_{10}H_{18}O$	0.05
18	13.45	Octyl acetate	172	1919	$\mathbf{C_{10}H_{20}O_2}$	46.46
19	14.21	D-Carvone	150	1976	$C_{10}H_{14}O$	0.13
20	14.61	1-Decanol	158	2031	$C_{10}H_{22}O$	0.04
21	15.59	Myrtenal	150	2194	$C_{10}H_{14}O$	0.30
22	17.32	Neryl acetate	196	2509	$C_{12}H_{20}O_2$	0.22
23	17.83	Lavandulyl acetate	196	2654	$C_{12}H_{20}O_2$	0.47
24	18.50	cis-Nerolidol	222	2784	$C_{15}H_{26}O$	0.56
25	19.08	γ-Neoclovene	204	2807	$C_{15}H_{24}$	0.01
26	19.22	β-Bourbonene	204	2840	$C_{15}H_{24}$	0.01
27	19.68	cis-β-Farnesene	204	2925	$C_{15}H_{24}$	0.03
28	23.76	(E)-β-Caryophyllene	204	3623	$C_{15}H_{24}$	0.27
29	27.64	Decyl oxirane	184	4303	$C_{12}H_{24}O$	0.01
30	30.82	1-Octanol	130	4863	$C_8H_{18}O$	0.40
31	32.38	Farnesyl acetate	264	5128	$\mathbf{C_{17}H_{28}O_2}$	5.04
32	33.28	Geranyl acetate	196	5113	$C_{12}H_{20}O_2$	0.25
33	34.47	Gurjunene	204	5523	$\mathbf{C_{15}H_{24}}$	2.46
34	36.16	Ricinelaidic acid lactone	280	5739	$C_{18}H_{32}O_2$	1.36
35	37.42	(−)-Serratol	290	6013	$C_{20}H_{34}O$	0.34
36	37.83	Incensole	306	6103	$C_{20}H_{34}O_2$	1.07
37	38.08	Incensyl acetate	348	6176	$C_{22}H_{36}O_3$	1.33
38	38.83	Incensole oxide	322	6247	$C_{20}H_{34}O$	0.35
39	39.54	Incensole oxide acetate	348	6413	$C_{22}H_{36}O_3$	0.50
40	40.88	γ-Stearolactone	282.5	6626	$C_{18}H_{34}O_2$	0.41
41	41.10	2-Tetradecanol	214.2	6666	$C_{14}H_{30}O$	0.28
2	42.11	3-Tridecanol	200.3	6838	$\mathbf{C_{13}H_{28}O}$	2.31
43	42.36	α-Cadinene	204	6930	$\mathbf{C_{15}H_{24}}$	3.54
44	42.84	γ-Cadinene	204	7021	$C_{15}H_{24}$	1.98
45	43.37	γ-Muurolene	204	7152	$C_{15}H_{24}$	1.90
46	44.13	Cadalene	198	7269	$C_{15}H_{18}$	2.81
47	45.32	Heptadecane	240.5	7456	$C_{17}H_{36}$	0.96
Oxygenated compounds						66.61
Non-oxygenated compounds						27.79

Table 1 (continued)

Peak no.	RT	Name	MS (M/e)			Area %
			M/Z	No scans	Chemical formula	
Total identification						94.4

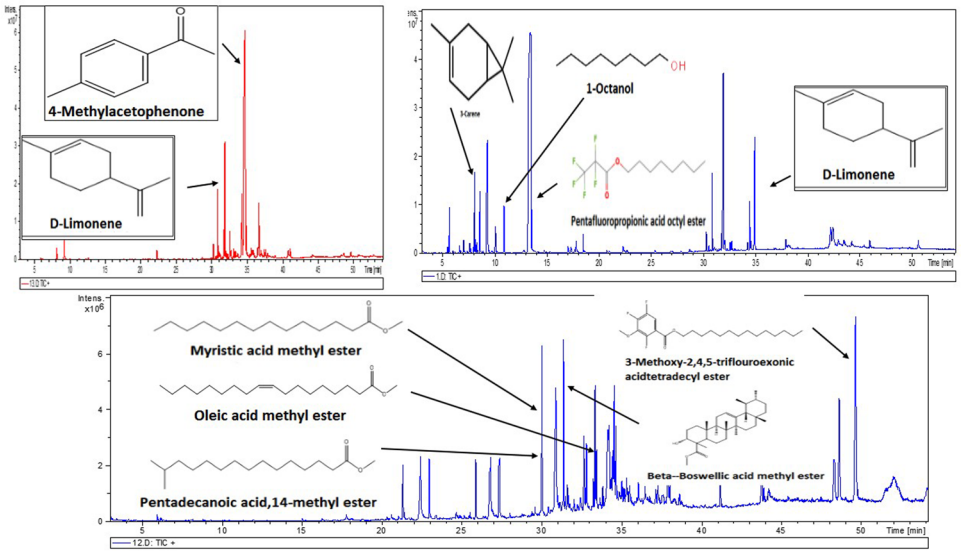

Fig. 1 **a** TIC chromatogram of the volatile oil BC resins, **b** TIC chromatogram of the saponification fixed oil BC resins, **c** TIC chromatogram of the Unsaponification fixed oil of Boswellia Carterri fruits

spherical shape and uniform in size (Trotta et al. 2008). Table 5 lists the components of the four formulations as well as the conclusions drawn from the evaluation of the responses. The formation and functionality of NSs are influenced by the kind of polymer used in their manufacture. Similar to the combination formed between the polymer and the crosslinker, the cavity size should be enough for conveying a drug molecule of a particular size (Selvamuthukumar et al. 2012).

Cyclodextrin-based Nano sponges have gained popularity recently due to their unique properties. By forming inclusion complexes through the inner nanocavities of cyclodextrins and non-inclusion complexes through the gaps in the sponges' cross-linked polymeric network, these sponges specifically increase the stability and apparent solubility of medicines. NSs made with cyclodextrins (like HPβ-CD) can offer a promising class of cross-linked polymers with a remarkable three-dimensional architecture made of both hydrophilic and hydrophobic nanosized pores that can successfully encapsulate a variety of drugs and increase the solubility of drugs that aren't very soluble (Swaminathan et al. 2009). Additionally, they have been shown to be secure for use with various administration methods, making them a viable drug delivery strategy (Vyas et al. 2008a, b). To increase the effectiveness of the drug loading and solubilization, the ratio of cyclodextrin to cross-linker can be adjusted during the manufacture of NSs. In the current investigation, DEX NSs was made using HPβ-CD as the polymer and DPC as the crosslinker in various ratios (1:1, 1:3, 1:4, and 1:6). In all the formulations that were looked into, NSs were prepared effectively.

Encapsulation efficiency

Table 5 shows the EE% values for all DEX NSs formulations. The EE% values for all formulations ranged from 99.15 ± 3.50 to 100% ± 4.76%. It was clear that all prepared NSs had high encapsulation efficiency (EE%), confirming the success of DEX NS preparation. The high EE% of the produced NSs could be attributed to optimal cross-linking between HPβ-CD and DPC, allowing for high inclusion of DEX salt in the NSs matrix and cyclodextrin cavity (Olteanu et al. 2014; Kumar et al. 2018). Along with the inclusion of DEX salt in the porous matrix of the Nano sponge, Additionally, it is responsible for completely trapping the drug molecules as an inclusion complex inside the hydrophobic host cyclodextrins' cavities, which are encircled by hydrophilic nanochannels (Trotta et al. 2012; Kumar et al. 2021).

Vesicle size, polydispersity index and zeta potential

The analysis of DEX NSs revealed that all produced NSs were in the nanosized range, with formulation sizes ranging from 59.9 ± 26.3 to 159.2 ± 20.2 nm (Table 5). Since the increase in cross linking agent molar ratio resulted in greater PS, it was discovered that formulations with a

Table 2 The main constituents of saponification fixed oil BC resin

List of fatty acid methyl ester and triterpenes			MS (M/e)			Area sum %
Peak no.	RT	Name	M/Z	No scans	Chemical formula	
1	15.429	15-Tetracosenoic acid	366	2167	$C_{24}H_{46}O_2$	0.03
2	16.282	Palmitic acid	256	2344	$C_{16}H_{32}O_2$	0.36
4	17.792	4-Ethylbenzoic acid	150	2614	$C_9H_{10}O_2$	0.66
5	18.118	Octanoic acid	144	2668	$C_8H_{16}O_2$	0.36
6	20.596	Dodecanedioic acid	230	3119	$C_{12}H_{22}O_4$	0.56
7	21.311	Lauric acid	200	3239	$C_{12}H_{24}O_2$	2.81
8	24.144	Nonahexacontanoic acid	999.8	3692	$C_{69}H_{138}O_2$	0.17
9	24.275	Amobarbital	226.2	3714	$C_{11}H_{18}N_2O_3$	0.08
10	25.145	2,8-Dimethylquinoline	157.2	3855	$C_{11}H_{11}N$	0.39
11	25.523	1,2-Cyclohexanedicarboxylic acid	452.7	3943	$C_8H_{12}O_4$	0.60
12	25.860	2-methyldodecanoic acid	214.3	4037	$C_{13}H_{26}O_2$	2.78
13	27.331	Undecanoic acid	186	4260	$C_{11}H_{22}O_2$	2.56
14	27.508	Stearic acid	284	4280	$C_{18}H_{36}O_2$	0.17
15	29.368	Myristoleic acid	226	4606	$C_{14}H_{26}O_2$	0.63
16	29.997	Myristic acid	228	4378	$C_{14}\mathbf{H_{28}O_2}$	8.89
17	31.319	11-Keto-beta-boswellic acid	470	4948	$C_{30}\mathbf{H_{46}O_4}$	8.31
18	31.445	β-Boswellic acid	456	4968	$C_{30}\mathbf{H_{48}O_3}$	10.21
19	33.190	Linolenic acid	278	5269	$C_{18}H_{30}O_2$	2.42
20	33.402	Petroselinic acid	282	5320	$C_{18}H_{34}O_2$	3.38
21	33.768	16-Methylheptadecanoic acid	284	5381	$C_{18}H_{36}O_2$	1.90
22	34.506	Oleic acid	282	5501	$C_{18}\mathbf{H_{34}O_2}$	10.05
23	34.615	Nonadecanoic acid	298	5529	$C_{19}H_{38}O_2$	4.84
24	34.792	7-Nonenamide	155.2	5561	$C_9H_{17}NO$	2.92
25	35.256	7-octenoic acid	142	5644	$C_8\mathbf{H_{14}O_2}$	3.44
26	36.000	Isovaleric acid	102	5784	C5H10O2	5.42
27	37.842	9-Octadecenamide, (Z)-	281	6089	$C_{18}H_{35}NO$	4.40
28	38.254	Octadecanamide	283	6189	$C_{18}H_{37}NO$	3.36
29	38.689	2,6-Pyridinedicarboxylic acid	181.1	6256	$C_7H_5NO_4$	1.38
30	42.225	2-formyl-butyric acid	116	6876	$C_5H_8O_3$	1.24
31	48.514	3-O-acetyl-β-boswellic acid	472.6	7995	$C_{32}H_{50}O_4$	8.98
32	53.280	2-carboxyethyl-3-cyano-5-methylhexanoic acid	255	8797	$C_{13}H_{21}NO_4$	0.1
33	53.629	2-ethoxycarbonyl-3-propylhexanoic acid	230	8852	$C_{12}H_{22}O_4$	0.22
Total identification						93.62

higher molar ratio of cross-linker had larger Vesicle diameters than those with a lower molar ratio of cross-linker (Yaşayan et al. 2020). Additionally, the data supported low polydispersity index (PDI) values of 0.265 to 0.675, indicating a uniform and constrained vesicle size distribution.

Table 5 further demonstrates that all of the formulations under investigation displayed a negatively charged zeta potential, which may have been caused by the free hydroxyl groups in HP β-CD and the carbonyl groups in DPC (Zidan et al. 2018; Omar et al. 2020). Absolute ZP values of greater than 20 were found for all formulations under consideration, and these values are more than sufficient to keep the individual particles apart from one another due to electrostatic repulsion. In contrast it keeps the stability of the prepared formulations (Abou Taleb et al. 2022).

Selection of the optimized DEX salt and oil NSs formulations

According to EE%, PS, PDI and ZP results, the best molar ratio between HPβ-CD and DPC was selected as the optimized ratio to prepare DEX salt NSs (1:6) (D4). The same molar ratio HPβ-CD: DPC (1:6), was used to prepare mixed oil extract NSs (O1). The λ_{max} of the oil extract was found to be at 233 nm. The EE%, PS, PDI and ZP of the new oil formulation were estimated and demonstrated in Table 5. It was found that the new oil Ns formulation

Table 3 The unsaponification fixed oil of *Boswellia Carterri* fruits

Peak no.	Unsaponification		MS (M/e)		Area sum %
	RT	Name	M/Z	Chemical formula	
1	3.516	2,3,4-trimethylhexane	128	C_9H_{20}	0.10
2	4.208	4-methyloctane	128	C_9H_{20}	0.10
4	6.011	4-ethylheptane	128	C_9H_{20}	0.51
5	6.766	3-Carene	136	$C_{10}H_{16}$	0.10
6	8.860	4-ethyldecane	170	$C_{12}H_{26}$	0.10
7	9.278	D-Limonene	**136**	$\mathbf{C_{10}H_{16}}$	**6.41**
8	9.782	Pentylcyclopropane	112	C_8H_{16}	0.30
9	12.013	2,3,3-trimethyl-1,4-Pentadiene	110	C_8H_{14}	0.20
10	20.596	Octacosane	394	$C_{28}H_{58}$	3.03
11	23.039	Hexadecane	226	$C_{16}H_{34}$	0.20
12	25.282	Heptadecane	240	$C_{17}H_{36}$	0.30
13	25.523	Hentriacontane	436	$C_{31}H_{64}$	0.61
14	25.711	3-Ethyl-3-methylheptane	142	$C_{10}H_{22}$	0.10
15	26.455	7,9-dimethylhexadecane	254	$C_{18}H_{38}$	0.30
16	26.965	2-methyloctacosane	408	$C_{29}H_{60}$	0.10
17	28.424	Tridecane	184	$C_{13}H_{28}$	0.10
18	29.293	Pentadecane	212	$C_{15}H_{32}$	0.30
19	30.821	Squalene	410	$C_{30}H_{50}$	20.00
20	33.821	4′-Methylacetophenone	134	$C_9H_{10}\mathbf{O}$	47.11
21	36.836	Campesterol	400	$C_{28}H_{48}\mathbf{O}$	10.15
22	38.592	Stigmasterol	412	$C_{29}H_{48}\mathbf{O}$	2.72
23	43.884	β.sitosterol	414	$C_{29}H_{50}\mathbf{O}$	3.64
Total					96.48

exhibited high EE%, with particle size in the nano range, low PDI and suitable ZP value.

Characterization of the optimized formulations

Surface morphology

Transmission electron microscopy (TEM) Figure 3a depicts the morphology of DEX and Oil NSs. The NSs are round and uniform, with no drug crystals on the surface. According to the figures, the NSs created using the ultrasonic- assisted processes have a uniform size distribution, crystallinity, and a porous character (Mahalingam et al. 2017).

Scanning electron microscopy (SEM) The SEM images of DEX and Oil NSs are illustrated in Fig. 3b. SEM analysis of the prepared NSs revealed nano-sized spherical particles having multiple pores on their surface (Muqtader et al. 2021). There were no residual crystals from the drugs indicating the complete encapsulation of drugs in the polymer (Sharma et al. 2011).

X-ray diffraction

The crystallinity of the Nano sponge formulations was determined using powder XRD. A diffractogram's peak position (angle of diffraction) is used to determine a crystal structure, and the number of peaks is used to assess sample crystallinity. The creation of an amorphous state indicates that the medication was diffused molecularly with CD (Patel and Rajput 2009). X-ray diffractometer plots of HPβ-CD, DPC, DEX Salt, Oil Extract and optimized NSs formulations (D4 and O1) are existing in Fig. 4a. The HPβ-CD diffractogram reveals the presence of two big diffraction peaks at 10.5° and 19.5° (Han et al. 2020), they lack structure but disclose the presence of a distant disorganized crystal structure and its amorphous nature (Nikolić et al. 2013; Paczkowska-Walendowska et al. 2020). DPC diffractometer showed sharp peaks as an indication on its crystallinity nature. DEX Salt and BO extract diffractometers showed that the drugs are crystalline, and have a polymorphic form with distinct sharp peaks (Qnouch et al. 2021).

Compared to the pure pharmaceuticals, the drug-loaded Nano sponges (D4 and O1) diffractometers demonstrated

Table 4 Lipidomic profiles of listed compounds by LC-MSMS

No.	RT	Compounds names	Chemical formula	Mass		Δ ppm	Ref	SMILES
				Measured &calculated	Exact mass of $[M-H]^-$			
1	8.15	FA 18:1;3O (E)-5,8,12-trihydroxyoctadec-9-enoic acid	$C_{18}H_{34}O_5$	329.2317, 329.2323	243.1592[$C_{13}H_{23}O_4$], 225.1492[$C_{13}H_{21}O_3$]	− 1.6117	$&*	O=C(O)CCCC(O)CCC(O)C=CCC(O)CCCCCC
2	8.80	FA 18:2;3O (10E,15E)-9,12,13-trihydroxyoctadeca-10,15-dienoic acid	$C_{18}H_{32}O_5$	327.2179, 327.2166	285.1707[$C_{15}H_{25}O_5$], 241.1801[$C_{14}H_{25}O_3$]	3.9575	$&*	O=C(O)CCCCCCCC(O)C=CC(O)C(O)CC=CCC
3	10.58	FA 15:3;O (6E,9E,12E)-8-hydroxypentadeca-6,9,12-trienoic acid	$C_{15}H_{24}O_3$	251.1651, 251.1642	207.1743[$C_{14}H_{23}O$]	3.8203	$&*	O=C(O)CCCCC=CC(O)C=CCC=CCC
4	10.99	FA 16:4;O (4E,7E,10E,13E)-3-hydroxyhexadeca-4,7,10,13-tetraenoic acid	$C_{16}H_{24}O_3$	263.1652, 263.1642	203.1435[$C_{14}H_{19}O$]	3.8780	$&*	O=C(O)CC(O)C=CCC=CCC=CCC=CCC
5	10.96	FA 15:4;O (3E,6E,9E,12E)-15-hydroxypentadeca-3,6,9,12-tetraenoic acid	$C_{15}H_{22}O_3$	249.1495, 249.1485	221.1176[$C_{13}H_{17}O_3$]	3.9518	$&*	O=C(O)CC=CCC=CCC=CCC=CCCO
6	10.94	ST 24:1;O4 R)-4-((3R,5S,7S,8R,9S,10S,13R,14S,17R) -3,7-dihydroxy-10,13-dimethylhexadecahydro-1H-cyclopenta[a]phenanthren-17-yl)pentanoic acid	$C_{24}H_{40}O_4$	391.2479, 391.2479	–	− 0.0163	$&*	C[C@H](CCC(=O)O)[C@H]1CC[C@@H]2[C@@]1(CC[C@H]3[C@H]2[C@H](C[C@H]4[C@@]3(CC[C@H](C4)O)C)O)C
7	11.32	FA 16:1;2O (E)-8,16-dihydroxyhexadec-9-enoic acid	$C_{16}H_{30}O_4$	285.2073, 285.2060	267.1950[$C_{16}H_{27}O_3$]	4.4530	$&*	O=C(O)CCCCCCC(O)C=CCCCCCCO
8	11.44	FA 18:4;O (6E,9E,12E,15E)-5-hydroxyoctadeca-6,9,12,15-tetraenoic acid	$C_{18}H_{28}O_3$	291.1966, 291.1955	263.1653[$C_{16}H_{23}O_3$]	3.9614	$&*	O=C(O)CCCC(O)C=CCC=CCC=CCC=CCC
9	11.64	FA 14:1;2O (E)-8,14-dihydroxytetradec-9-enoic acid	$C_{14}H_{26}O_4$	257.1759, 257.1747	239.1652[$C_{14}H_{23}O_3$]	4.6586	$&*	O=C(O)CCCCCCC(O)C=CCCCCO
10	11.77	11-keto-ursolic acid	$C_{30}H_{46}O_4$	469.3324, 469.3312	407.3324[$C_{29}H_{43}O$], 373.2744[$C_{24}H_{34}O_3$]	2.5390	@*	CC1CCC2(CCC3(C(=CC(=O)C4C3(CCC5C4(CCC(C5(C)C)O)C)C)C2C1C)C)C(=O)O
11	11.81	FA 16:0;2O 8,16-dihydroxyhexadecanoic acid	$C_{16}H_{32}O_4$	287.2232, 287.2217	269.2129[$C_{16}H_{29}O_3$]	5.1845	$&*	O=C(O)CCCCCCC(O)CCCCCCCCO
12	12.09	FA 20:3;4O (11E,14E,17E)-6,9,10,20-tetrahydroxyicosa-11,14,17-trienoic acid	$C_{20}H_{34}O_6$	369.2284, 369.2272	–	3.3268	$&*	O=C(O)CCCCC(O)CCC(O)C(O)C=CCC=CCC=CCCO

Table 4 (continued)

No.	RT	Compounds names	Chemical formula	Mass		Δ ppm	Ref	SMILES
				Measured &calculated	Exact mass of $[M-H]^-$			
13	12.51	FA 18:1;3O (E)-5,8,12-trihydroxyoctadec-9-enoic acid	$C_{18}H_{34}O_5$	329.2327, 329.2323	285.1837[$C_{19}H_{25}O_2$], 201.1119[$C_{10}H_{17}O_4$]	1.4472	$&*	O=C(O)CCCC(O)CCC(O)C=CCC(O)CCCCCC
14	12.23	(E)-10-hydroxyicos-11-enoic acid	$C_{20}H_{38}O_3$	325.2748, 325.2748		− 2.4594	%	O=C(O)CCCCCCCCC(O)C=CCCCCCCCC
15	12.57	FA 18:1;2O (E)-7,10-dihydroxyoctadec-8-enoic acid	$C_{18}H_{34}O_4$	313.2383, 313.2373	295.2285[$C_{18}H_{31}O_3$]	3.0177	$&*	O=C(O)CCCCCC(O)C=CC(O)CCCCCCCC
16	12.70	LPA 16:0 2-hydroxy-3-(phosphonooxy)propyl palmitate	$C_{19}H_{39}O_7P$	409.2360, 409.2371	125.9947[$C_3H_6O_5P$]	2.6879	$&*	O=C(OCC(O)COP(=O)(O)O)CCCCCCCCCCCCCCC
17	13.18	FA 20:5;O (5E,8E,11E,14E,17E)-7-hydroxyicosa-5,8,11,14,17-pentaenoic acid	$C_{20}H_{30}O_3$	317.2116, 317.2111	273.2225[$C_{19}H_{29}O$]	1.4410	$&*	O=C(O)CCCC=CC(O)C=CCC=CCC=CCC=CCC
18	13.37	FA 20:4;2O (8E,11E,14E,17E)-6,7-dihydroxyicosa-8,11,14,17-tetraenoic acid	$C_{20}H_{32}O_4$	335.2211, 335.2217	291.2338[$C_{19}H_{31}O_2$]	− 1.6573	$&*	O=C(O)CCCCC(O)C(O)C=CCC=CCC=CCC=CCC
19	14.4	(E)-2-hydroxynonadec-9-enoic acid	$C_{19}H_{36}O_3$	311.2591, 311.2590		− 0.3212	%	O=C(O)C(O)CCCCCCC=CCCCCCCCCC
20	14.60	FA 16:2;O (9E,12E)-8-hydroxyhexadeca-9,12-dienoic acid	$C_{16}H_{28}O_3$	267.1955, 267.1955	223.2060[$C_{15}H_{27}O$], 169.1586[$C_{11}H_{21}O$]	− 0.0229	$&*	O=C(O)CCCCCCC(O)C=CCC=CCCC
21	14.63	FAHFA (5E,8E,11E,14E)-4-((8E,11E)-pentadeca-8,11-dienoyloxy) heptadeca-5,8,11,14-tetraenoic acid	$C_{32}H_{50}O_4$	497.3692, 497.3684	–	1.5312	%	O=C(O)CCC(OC(=O)CCCCCCC=CCC=CCCCC)C=CCC=CCC=CCC=CCC
22	14.68	FA 18:3;O (9E,12E,15E)-8-hydroxyoctadeca-9,12,15-trienoic acid	$C_{18}H_{30}O_3$	293.2122, 293.2111	249.2213[$C_{17}H_{29}O$]	3.7446	$&*	O=C(O)CCCCCCC(O)C=CCC=CCC=CCC
23	14.81	FA 16:1;O (E)-8-hydroxyhexadec-9-enoic acid	$C_{16}H_{30}O_3$	269.2123, 269.2111	251.2009[$C_{16}H_{27}O_2$]	4.5139	$&*	O=C(O)CCCCCCC(O)C=CCCCCCC
24	14.87	FA 18:1;O (E)-8-hydroxyoctadec-9-enoic acid	$C_{18}H_{34}O_3$	297.2436, 297.2424	279.2331[$C_{18}H_{31}O_2$]	3.9359	$&*	O=C(O)CCCCCCC(O)C=CCCCCCCCC
25	15.41	FA 12:0Bronsted acid	$C_{12}H_{24}O_2$	199.1696, 199.1693	184.0013	1.8852	$&*	O=C(O)CCCCCCCCCCC
26	15.33	FA 13:1 Isotridecenoic acid	$C_{13}H_{24}O_2$	211.1697, 2,111,693	171.2430	2.2116	$&*	O=C(O)CCCCCCCC=CCCC
27	**15.42**	FA 14:0;(2OH) 2-hydroxytetradecanoic acid	$C_{14}H_{28}O_3$	243.1966, 243.1955	197.1906[$C_{13}H_{25}O$]	4.7433	$&*	O=C(O)C(O)CCCCCCCCCCCC

Table 4 (continued)

No.	RT	Compounds names	Chemical formula	Mass		Δ ppm	Ref	SMILES
				Measured &calculated	Exact mass of $[M-H]^-$			
28	**15.60**	FA 18:0;(2OH) 2-hydroxyoctadecanoic acid	$C_{18}H_{36}O_3$	299.2592, 299.2581	281.2470[$C_{18}H_{33}O_2$]	3.7237	$&*	O=C(O)C(O)CCCCCCCCCCCCCCCC
29	**15.97**	FAHFA 19:4;O (4E,7E,10E,13E)-3-(propionyloxy) hexadeca-4,7,10,13-tetraenoic acid	$C_{19}H_{28}O_4$	319.1921, 319.1904	277.1811[$C_{17}H_{25}O_3$]	5.3959	$&*	O=C(O)CC(OC(=O)CC) C=CCC=CCC=CCC=CCC
30	**16.19**	FA 14:1 Myristoleic acid	$C_{14}H_{26}O_2$	225.1855, 225.1849	179.0848	2.7785		O=C(O)CCCCCCCC=CCCCC
31	16.56	FA 20:5 (5E,8E,11E,14E,17E)-icosa-5,8,11,14,17-pentaenoic acid	$C_{20}H_{30}O_2$	301.2185, 301.2162	–	− 1.2827	$&*	O=C(O) CCCC=CCC=CCC=CCC=CCC=CCC
32	17.00	LPA 18:2 (9E,12E)-2-hydroxy-3-(phosphonooxy)propyl octadeca-9,12-dienoate	$C_{21}H_{39}O_7P$	433.2360, 433.2365	–	1.1541	$&*	O=C(OCC(O)COP(=O)(O)O)CCCCCC CC=CCC=CCCCCC
33	17.07	FA 14:0 Myristic acid	$C_{14}H_{28}O_2$	227.2012, 227. 2006	158.1427[$C_9H_{18}O_2$]	2.9095	$*@	O=C(O)CCCCCCCCCCCCC
34	17.11	FA 15:1 (E)-pentadec-9-enoic acid	$C_{15}H_{28}O_2$	239.2014, 239.2006	192.0593[$C_{14}H_{18}O$]	3.3377	$*@	O=C(O)CCCCCCCC=CCCCCC
35	17.14	FA 18:3 a-Linolenic acid	$C_{18}H_{30}O_2$	277.2173, 277.2162	259.2068[$C_{18}H_{27}O$], 233.1534[$C_{15}H_{21}O_2$]	3.8904	$@	O=C(O)CCCCCCCC=CCC=CCC=CCC
36	17.16	FA 16:0;(2OH) 8-hydroxyhexadecanoic acid	$C_{16}H_{32}O_3$	271.2280, 271.2268	225.2220[$C_{15}H_{29}O$], 59.0222[C_2H_3O]	4.6308	$&*	O=C(O)CCCCCCC(O)CCCCCCCC
37	17.50	FA 16:1 Palmitoleic acid	$C_{16}H_{30}O_2$	253.2172, 253.2162	253.2172[$C_{16}H_{27}O$]	3.8976	$@	O=C(O)CCCCCCCC=CCCCCCC
38	17.86	FA 15:0 Sarcinic acid	$C_{15}H_{30}O_2$	241.2171, 241.2162	145.1589[C9H21O]	3.6487	$@	O=C(O)CCCCCCCCCCCCCC
39	18.05	FA 18:2 Linoleic acid	$C_{18}H_{32}O_2$	279.2330, 279.2319	261.2214[$C_{18}H_{29}O$]	4.2097	$@	O=C(O)CCCCCCCC=CCC=CCCCCC
40	18.43	FA 16:0 Palmitic acid	$C_{16}H_{32}O_2$	255.2328, 255.2319	138.1155[$C_9H_{14}O$]	3.5295	$@	O=C(O)CCCCCCCCCCCCCCC
41	18.68	3-Oxo-7,24-dienetirucallic acid	$C_{30}H_{46}O_3$	453.3379, 453.3363	371.2619[$C_{24}H_{35}O_3$], 267.0790[$C_{20}H_{11}O$]	3.4607	@	CC(=CCCC(C1CCC2(C1(CCC3=C2CC C4C3(CCC(=O)C4(C)C)C)C)C)C(=O) O)C
42	19.22	FA 18:1 Oleic acid[4]	$C_{18}H_{34}O_2$	281.2487, 281.2475	–	4.1990	@$	O=C(O)CCCCCCCC=CCCCCCCCC
43	19.36	FA 20:2 (11E,14E)-icosa-11,14-dienoic acid	$C_{20}H_{36}O_2$	307.2646, 307.2636	212.1419[$C_{12}H_{30}O_3$]	4.5564	@$	O=C(O)CCCCCCCCCC=CCC=CCC CCC

Table 4 (continued)

No.	RT	Compounds names	Chemical formula	Mass		Δ ppm	Ref	SMILES
				Measured &calculated	Exact mass of $[M-H]^-$			
44	19.53	FA 19:1 cis-10-Nonadecenoic acid	$C_{19}H_{36}O_2$	295.2636, 295.2632	–	1.6409	@$	O=C(O)CCCCCCCC=CCCCCCCCC
45	19.55	Boswellic acid	$C_{30}H_{48}O_3$	455.3530, 455.3520	437.3430[$C_{30}H_{45}O_2$]	2.1840	@	–
46	20.02	FA 18:0 Stearic acid[4]	$C_{18}H_{36}O_2$	283.2643, 283.2632	–	3.9729	@$	O=C(O)CCCCCCCCCCCCCCCCC
47	20.13	FA 20:1 (E)-icos-11-enoic acid	$C_{20}H_{38}O_2$	309.2803, 309.2788	–	4.8404	$&*	O=C(O)CCCCCCCCCC=CCCCCCCCC
48	20.75	Norethisterone acetate	$C_{22}H_{28}O_3$	339.2000, 339.2013	183.0112	− 3.8373	$%	CC(=O)O[C@]1(CC[C@H]2[C@@H]3CCC4=CC(=O)CC[C@@H]4[C@H]3CC[C@]12C)C#C
49	21.92	FA 15:4 (3E,6E,9E,12E)-pentadeca-3,6,9,12-tetraenoic acid	$C_{15}H_{22}O_2$	233.1543, 233.1536	–	3.0268	$&*	O=C(O)CC=CCC=CCC=CCC=CCC
50	24.16	FA 15:3 (6E,9E,12E)-pentadeca-6,9,12-trienoic acid	$C_{15}H_{24}O_2$	235.1703, 235.1693	220.1465[$C_{14}H_{20}O_2$], 178.9902[$C_{11}H_{14}O_2$]	4.3866	$&*	O=C(O)CCCCC=CCC=CCC=CCC

Compounds listed in the Table were found in petroleum ether extract, (@) compounds compared with literature, (#) compounds identified from the KNApSAcK database, ($) compounds identified from MS_Dial, (&) compounds identified from Metlin, (*) compounds identified from RIKEN and (%) MsdialCytoscape

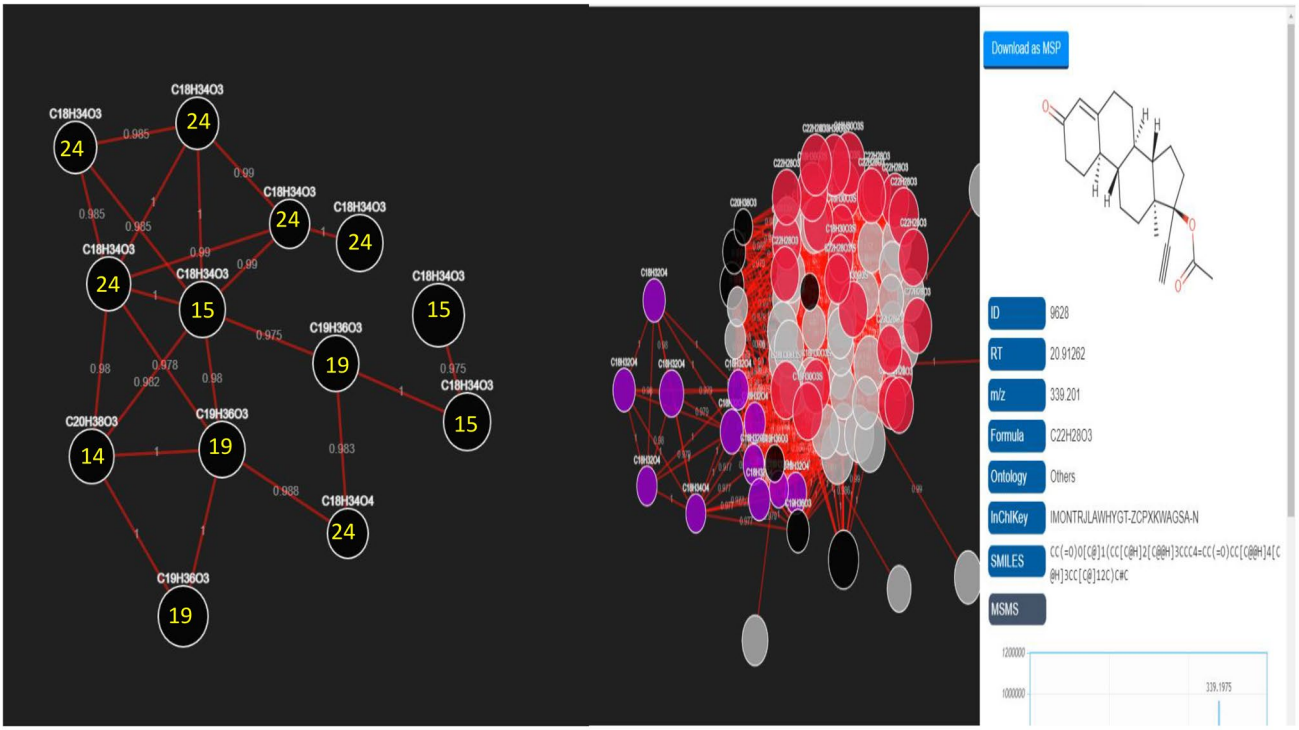

Fig. 2 Methods for the generation of molecular networks from lipidomic mass spectrometry using MS-DIAL (4.90) via data visualization then molecular spectrum networking data with the GNPS web platform for all signals compounds (15,19, 24 and 20) showed Norethisterone acetate compound

Table 5 Composition, entrapment efficiency and physico-chemical properties of DEX salt and oil extract NSs

Code	Drug (10 mg)	Molar ratio		EE% ± SD	VS ± SD	PDI	ZP ± SD
		2-Hydroxy propyl-β-cyclodextrin (2HP-β-CD)	Di-phenyl carbonate (DPC)				
D1	DEX	1	1	99.99 ± 0.20	59.9 ± 26.3	0.318	− 21.4 ± 2.36
D2		1	3	100 ± 0.30	66.1 ± 10.5	0.675	− 20.3 ± 1.45
D3		1	4	99.15 ± 3.50	66.9 ± 15.5	0.265	− 22.5 ± 2.54
D4		1	6	100% ± 4.76	159.2 ± 20.2	0.524	− 26.2 ± 6.26
O1	Oil	1	6	100% ± 3.06	229.2 ± 30.23	0.596	− 25.1 ± 3.86

a weakening or elimination of powerful peaks when diffractograms of individual components and NSs formulations were examined. This reveals unequivocally how drug dispersion in NS polymer causes crystals to change into amorphous form. The polymeric enclosing layers constrain the drug film, which prevents crystallization at the air–solid junction. As a result, the coating layer includes an additional solid–solid barrier. This is known as an amorphous solid dispersion, and it is almost probably the result of drug-polymer interactions developing as a result of the drug's crystal lattice's intermolecular connections being broken down (Almutairy et al. 2021). This confirmed that medicines were entirely incorporated into the cavity of 2HPβ-CD, and the success of Nano sponge fabrication (Ansari et al. 2011a; Nikolić et al. 2013; Mahalingam et al. 2017).

Fourier transform infrared spectroscopy analysis

The interactions between pharmaceuticals and excipients were investigated by comparing the FTIR spectra of pure drugs with drug-loaded Nano sponges (D4 and O1) (Fig. 4b). The FTIR spectra of HP-β-CD showed prominent absorption bands at 3415 cm^{-1} (O–H stretching), 2929 cm^{-1} (C–H stretching), 1645 cm^{-1} (H–O–H bending), 1157 cm^{-1} (C–O stretching), and 1031 cm^{-1} (C–O–C stretching) (Gidwani and Vyas 2015; Han et al. 2020). FTIR spectrum bands for DPC revealed distinctive

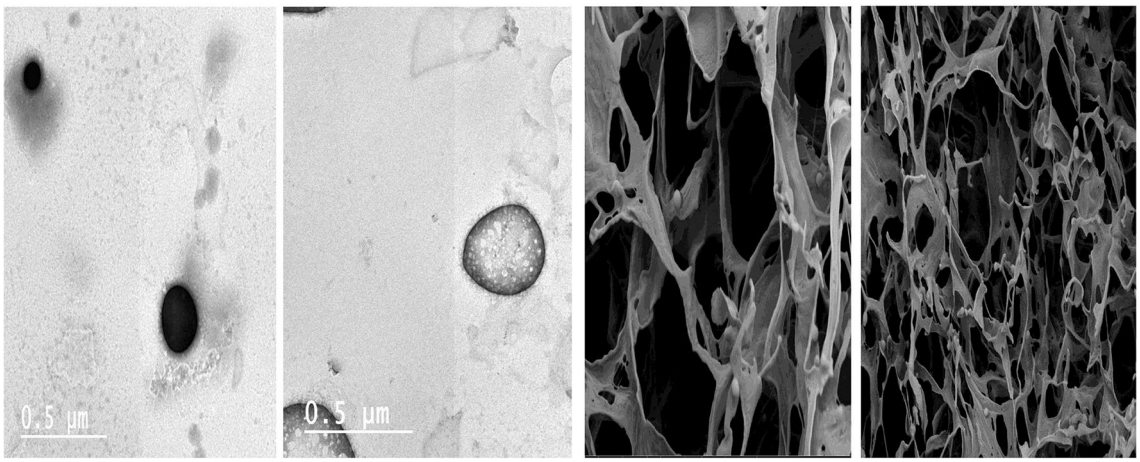

Fig. 3 **a** TEM micrographs of Nano sponges optimized formulations (D4 and O1), **b** SEM micrographs of Nano sponges optimized formulations (D4 and O1)

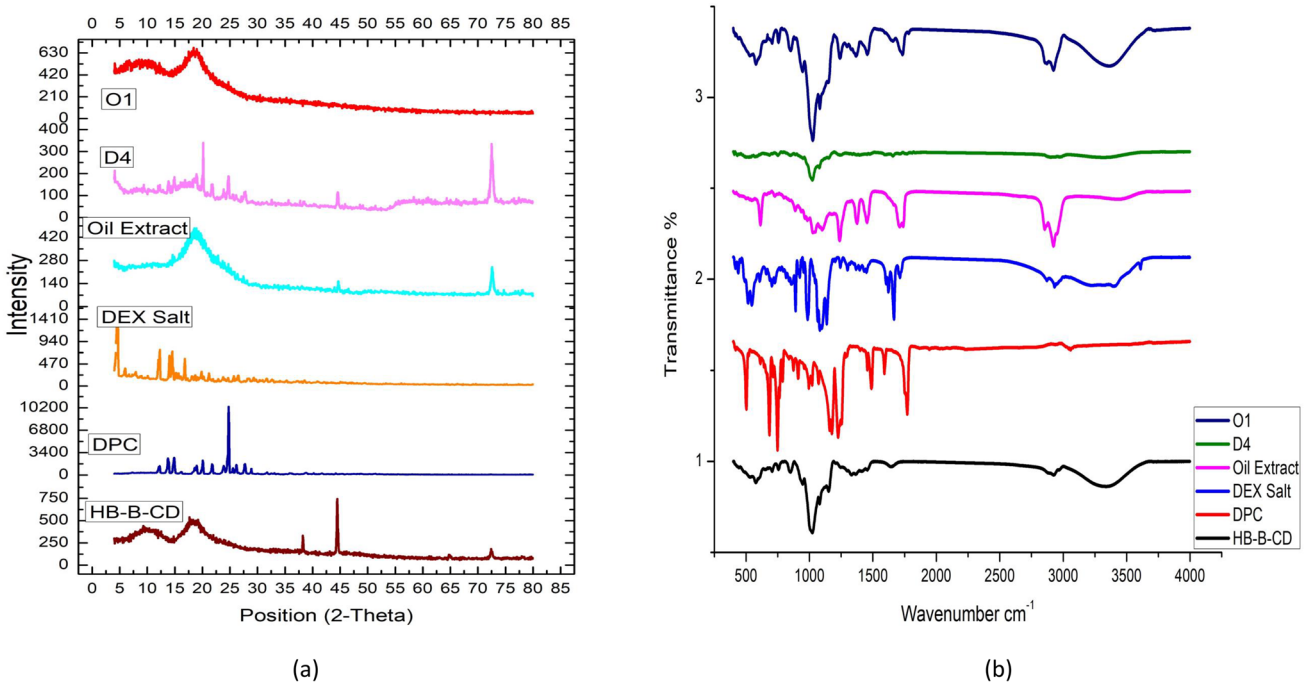

Fig. 4 **a** X-Ray diffractometer of different Nano sponges components and optimized formulations, **b** IR spectrum of different Nano sponges components and optimized formulations

absorbance band at 1753 cm^{-1} for carbonate bond (Dubey et al. 2017). DEX exhibited distinct absorbance bands at 1706, 1660, and 1616 cm^{-1}, which were attributed to –C=O stretching vibrations connected to C3-cyclic and C20 carbonyl groups, as well as double bond context coupled to –C=O bonds. Furthermore, two more different absorption bands of 3468 cm^{-1} and 1270 cm^{-1} were realized due to the stretching ambiences of the O–H and C–F bonds, respectively (Rodrigues et al. 2009; Long et al. 2019).

The IR spectrum of BO extract is comparative to Boswellia acids and it displayed characteristic peaks at 3437 cm^{-1} (OH stretching), 2932 cm^{-1} (C-H stretching), 1697 cm^{-1} (C=O stretching of aryl acid), 1453 cm^{-1} (C–H bend),

1375 cm^{-1} (COO symmetric stretching of carboxylates), 1240 cm^{-1} (C–CO–C stretching of aryl ketone), 1025 cm^{-1} and 988 cm^{-1} (ring structures of cyclohexane) (Mehta et al. 2016).

In the distinctive peaks of DEX or Oil extract, the IR spectrum of the optimized Nano sponge formulations (D4 and O1) revealed a shifting and diminished intensity. This shift in the characteristic peaks may be explained by the presence of physical interactions between drugs and various NS elements, such as Van der Wall bonds, hydrogen bonds, or dipole interactions, without any chemical changes to the drugs' structure after encapsulation, which can result in the best possible entrapment of DEX or Oil in Nano sponges (Mazyed and Zakaria 2019; Omar et al. 2020; Younis et al. 2023).

In-vitro release study

CD-based NSs can be a valuable technique for delivering medications in a sustained manner. Drug encapsulation in a cross-linked NSs structure allows for prolonged drug administration, lower doses, fewer side effects, and changed pharmacokinetics. These characteristics can be used to improve medicine distribution (Osmani et al. 2018).

The produced NSs formulations and the free drug solutions' DEX salt and Oil extract release profiles were shown in Fig. 5. The release profiles of the tested formulations displayed a biphasic behavior, with an initial quick-release lasting for the first six hours. This first rapid release may have been caused by the drug's adsorption on the NSs' surface vesicles, which led to a fast release from NSs (Sunil et al. 2019). Followed by a delayed, slow release for 24 h. On the other hand, about 100% of DEX salt and oil extract were liberated from the free drug solution after 6 h (Fig. 6).

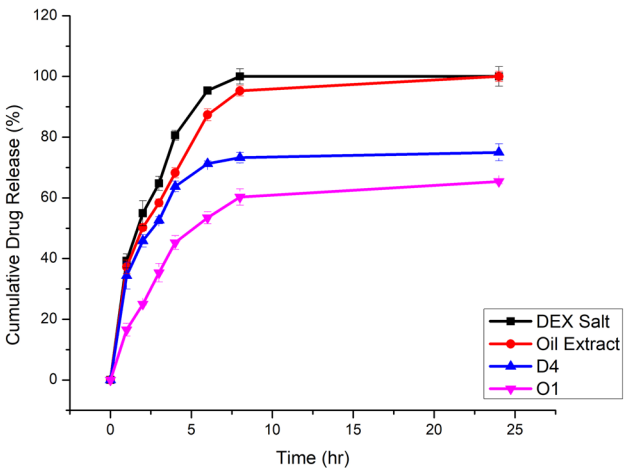

Fig. 5 In-vitro release profiles of drugs from Nano sponges optimized formulations (D4 and O1)) and free drugs at PBS 7.4

Frequent administration is the main disadvantage of the majority of the traditional, commercially available drug delivery devices. The medication, however, is kept and released gradually over time after being loaded into the Nano sponge. It has been previously reported that hydrophilic cyclodextrin Nano sponges are used to adjust the drug release rate, as it facilitates medication absorption over biological barriers and it may help to protect the medication throughout its passage through the stomach (2008a, b; Abou Taleb et al. 2019).

NSs formulations' correlation coefficient (R^2) values showed better fitting to Higuchi's model than zero order and first order kinetic models, according to a linear regression analysis of the mathematical models used for release information gathered from NSs formulations (R^2 ranged from 0.8634 to 0.9865). The Peppas equation was used for further examination of the DEX and oil release process (Peppas and Sahlin 1989; Lokhande et al. 2013) when high linearity was observed. According to Peppas theory, if $n = 0.43$, drug release follows the Fickian diffusion process, $0.43 < n < 0.85$ follows anomalous (non-Fickian) diffusion, $n = 0.85$ follows case II transport, and $n > 0.85$ follows super-case II transport (Peppas and Sahlin 1989). Values of the release exponent "n" for NSs formulations ranged from 0.117 to 0.3568, respectively, indicating a Fickian diffusion-controlled release mechanism.

In-vivo pharmacological study

Effect of different formulations on inflammatory and allergic mediators of respiratory tract

Results in Table 6 revealed the biochemical analysis of the intercellular adhesion molecule-1 (ICAM-1), inflammatory marker Ilβ4, and the chemokine Leukotriene LTB_4. All indicators considerably increased in the positive control group compared to the negative control group. Intranasal instillation of different medications for treating allergic rhinitis in rats showed different effects on the levels of biological markers.

The function of ICAM-1, is crucial in the disease progression of the inflammatory allergic rhinitis. Its expression in epithelial cells of the nasal cavity during allergic rhinitis is considered the main feature of allergic reaction. It is used for the prognosis of the disease and evaluation of its severity (Bianco et al. 2000). In the case of ICAM-1, results showed that the effect of treatment on inhibition of its level were in the order of BO > D4 > O1, while treatment with free DEX elevated the levels of ICAM-1. The potent chemokine Leukotriene Ilβ4 is an allergic inflammatory marker that is a metabolite of arachidonic acid. It acts by enhancing the aggregation of neutrophils. When it is activated, it causes accumulation of inflammatory and immune effector cells

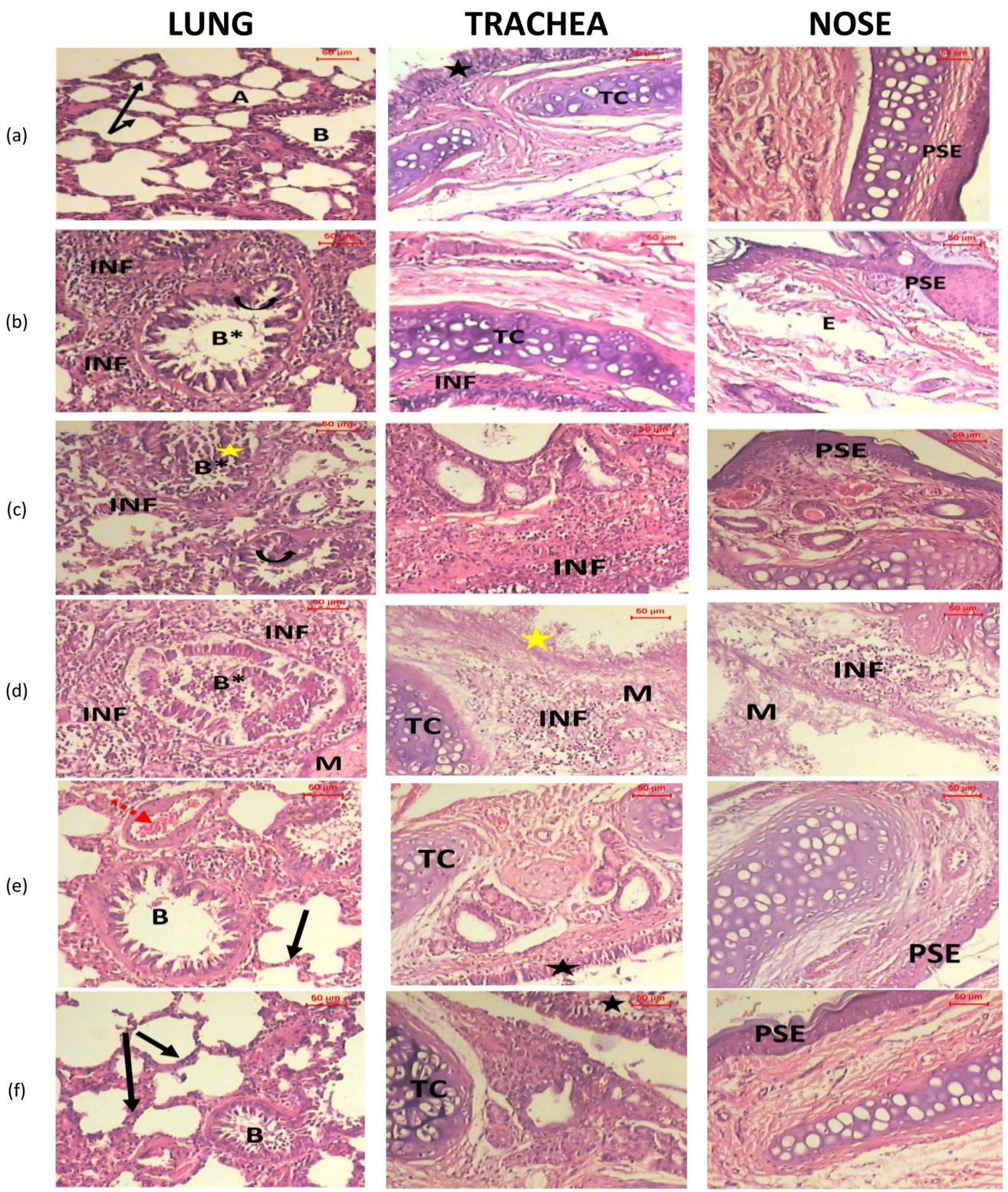

Fig. 6 Photomicrographs of lung, tracheal and nasal tissues of **a** Negative control, **b** Positive control, **c** Boswellia Oil, **d** DEX salt, **e** DEX salt Nano sponges (D4) and **f** Oil extract Nano sponges (O1). *Black arrows*; alveoli with average thickness wall, *Dashed red arrows*; congested blood vessels, *A*; Alveoli, *B*; bronchioles, *B**; bronchioles filled with mucus, *INF;* inflammatory cells infiltrates, *Black stars*; ciliated pseudostratified columnar epithelium, *Yellow stars*; hyperplastic columnar epithelium, *TC*; tracheal cartilage, *PSE*; pseudostratified epithelium. All photomicrographs were taken at two magnification powers (×200 and ×400)

Table 6 Effects of treatment with *Boswellia carterii* volatile oil, Dexa salt and their Nano Sponge formulations on inflammatory and allergic mediators of respiratory tract

Parameter			
Group	ICAM-1 (pg/ml)	Ilβ4 (pg/ml)	LTB_4(pg/ml)
Negative control	316 ± 10	1340 ± 5	2445 ± 4.42
Positive control	1192 ± 6.5[@]	4186 ± 55.5[@]	3543 ± 49.4[@]*
B. carterii oil	346.1 ± 40*	2085 ± 59.5*	1756 ± 39.56[@]*
Dexa salt	5810.71 ± 4.6[@]*	4348 ± 199.5[@]	4016 ± 12.61[@]*
DEX Ns (D4)	380.4 ± 9.6*	3207 ± 199.5[@]	3757 ± 36.78[@]
B. carterii Ns (O1)	838 ± 50[@]*	1430 ± 100.7*	2251 ± 12.25*

Result is expressed as means ± S.E. N = 8.Comparisons between means were carried out using one way analysis of variance (ANOVA) followed by Tukey Kramer's multiple comparisons test. $p \leq 0.001$

[@] Significantly different from Negative control

*Significantly different from positive control

in addition to its action on T cells in the immune response, leading to potentiation of the release of cytokines (Bocsan et al. 2021). Results showed that the effect of treatment on inhibition of the Ilβ4 level were in the order of O1 > BO > D4. Treatment with free DEX not enough of an appeal to make a difference on Ilβ4 levels. Leukotriene B_4 (LTB_4) is an important component of tissue injury and inflammation and a potent lipid mediator that is essential for the proliferation and recruiting of neutrophils (Asahara et al. 2022). Results showed that both BO and BO in Nano sponge have a significant effect on the inhibition of LTB_4 levels, while treatment with free DEX and DEX Nano sponge didn't appeal to have a significant effect on LTB_4 levels. In the present work, the best effects as a whole were those of *B. carterii* mixed oil, *B. carterii* mixed oil in Nano sponge (O1) and Dexa salt in Nano sponge (D4) as they reduced ICAM-1 and Ilβ4 levels significantly.

Different symptoms of inflammation include redness, heat, pain, swelling, and a reduction in function. Numerous inflammatory mediators like ICAM-1, Ilβ4 and LTB_4 are produced, which causes these symptoms to appear. It has been previously reported that, numerous medicinal plants such as *Boswellia* species have anti-inflammatory activity as Boswellic acids derived from them works on inhibiting the synthesis of prostaglandins by interfering with the cyclooxygenase system and the arachidonic acid cascade, which subsequently can inhibit the production of leukotrienes and thus can control the progress of inflammatory diseases like chronic asthma bronchitis and rhinitis (Ammon et al. 1993).

Results obtained on treatment with DEX salt can be explained in light of the study of Bocsan et al., who revealed that ICAM-1 levels were greater in patients sensitized with pollen grains and suffering allergic rhinitis, than non- sensitized individuals during pollen exposure. On the other hand, treatment with antihistaminic therapy didn't lower their levels in sera during pollen season (Bocsan et al. 2021). In a related investigation, Vestbo and associates prospectively tracked 290 individuals with mild to moderate chronic obstructive pulmonary disease (COPD) and discovered no variation in the pace of inflammatory mediator decrease. In this patient cohort, the rate of exacerbation did not reduce with the use of inhaled corticosteroids (ICS) (Vestbo et al. 1999). The results of the Lung Health Study in many aspects confirmed those previously reported on the lack of impact of ICS on lung function loss; nevertheless, there were beneficial side effects, such as reduced symptoms, fewer doctor visits, and less airway hyperreactivity (Wise et al. 2000). Loading of Dex in Nano sponges enhanced its therapeutic activity when compared to free drug, which may be rationalized by the sustained release of drug from Nano sponges that lead to prolonged activity and reduction of adverse effects (Shrestha and Bhattacharya 2020).

Histopathological examination

The Histopathological examinations of the lung, trachea and nose from different groups are illustrated in Fig. 6. The figures revealed that the lungs of negative control rats (Fig. 6a) are more like a well-organized sponge consisting of functional respiratory units alveoli. Each alveolus shares its wall (interalveolar septum) with adjacent alveoli they are average in thickness, bronchioles lined by columnar epithelium supported by smooth muscle layer have normal appearance, bronchial vessels have normal looking and average thickness, examination of tracheal tissue revealed that it is lined by ciliated, pseudostratified columnar epithelium, rests upon ordinary connective tissue, Incomplete rings of hyaline cartilage encircle the trachea and photomicrographs of nasal tissue revealed that the nasal cavity lined by pseudostratified epithelium (PSE) mucosa and submucosa region filled of blood vessels, mucin and serous secreting gland.

On the other hand the positive group tissue examinations (Fig. 6b), exhibited disturbed lung architecture and severe infiltration of lung tissue with inflammatory cells some with focal formation, indentation of bronchial lining with evidence of intrabronchial mucus presence, bronchial vessels are congested with increased thickness, the trachea is lined minimally destructed pseudostratified columnar epithelium infiltrated by inflammatory cells, nasal tissues showed disturbed mucosal region by edema and inflammatory cell infiltrate.

Histopathological examinations of tissues from the *B. carterii* mixed oil group (Fig. 6c) showed that the lung tissues are infiltrated with inflammatory cell infiltrates, especially around the bronchioles, which are filled with mucus and have indented walls. Histopathological examination of tracheal tissues revealed that the trachea is lined

by ciliated, pseudostratified columnar epithelium with severe inflammatory cells infiltrated.

Also, histopathological examination of the lung tissue DEX group (Fig. 6d) showed that the lung tissues were destroyed mainly by severe infiltration of inflammatory cells with focal areas of mucin formation. Histopathological examination of tracheal tissue revealed that the tracheal lining is destructed and rests upon connective tissue infiltrated by inflammatory cells and the focal regions of mucin. Also, histopathological examination of nasal tissue showed destruction of nasal tissue by inflammatory cells infiltrating and focal areas of mucin.

Histopathological examination of tissues treated with DEX salt in Nano sponges D4 (Fig. 6e) revealed that the tissues retained the normal appearance of lung architecture, with only the bronchial vessels congested with increased thickness. On the other hand, the lungs treated with *B. carterii* mixed oil in Nano sponge group O1 (Fig. 6f) are more like a well-organized sponge consisting of functional respiratory units alveoli; each alveolus shares its wall (interalveolar septum) with minimal inflammatory cells infiltrate, bronchioles lined by columnar epithelium supported by smooth muscle layer has normal appearance, bronchial vessels have normal looking and average thickness. Histopathological examination of nasal tissues treated with D4 and O1 revealed that the nasal cavity is lined by pseudostratified epithelium (PSE), mucosa, and submucosa region filled with blood vessels, mucin, and serous secreting gland, with improvement in the thickening of nasal cavity lining.

Results obtained with histopathological examinations were in accordance with that observed with inflammatory markers measurements. Since the antiallergic anti-inflammatory mechanism of action of conventional Boswellia oil and its Nano sponge formulation is the same as that adopted by non-steroidal anti-inflammatory drug Dexa salt, which acts by suppressing inflammation, via inhibiting eicosanoid synthesis (Koeberle et al. 2018), therefore it is suggested that the tested natural products in our study are potent anti-inflammatory and anti-allergic agents and can be promising for alleviating signs and symptoms of allergic rhinitis as they significantly lowered the inflammatory biomarkers ICAM-1, Ilβ4 and LTB_4 levels in comparison to free Dexa salt which can be attributed to sesquiterpenoids, diterpenes, and triterpenes present in Boswellia, particularly boswellic acids and other tirucallic acids. Moreover, Boswellic acids are pentacyclic triterpene acids that may be able to treat chronic conditions with an inflammatory component because they target cathepsin G and 5-lipoxygenase (5-LO) in neutrophils (Rainsford 2007; Siemoneit et al. 2009; Huang et al. 2022).

Conclusion

The successful extraction and characterization of volatile oil from *B. carterii* have been accomplished, and Nano sponges loaded with either *B. carterii* oil or Dex salt exhibits the most desirable characteristics essential for an effective dosage form. These Nano sponges, characterized by a small particle size, demonstrate continuous release profiles lasting up to 24 h. Moreover, they display a remarkable capacity to extend drug release duration, potentially leading to a reduction in drug administration frequency, lower medication dosages, and the avoidance of systemic adverse effects. Both *B. carterii* volatile oil, Dexa salt, and their nanoformulations (D4 and O1) were examined to evaluate the anti-inflammatory activity for treating respiratory allergies. Histopathologic examinations, along with measurements of Intracellular adhesion molecule-1 (ICAM-1), Leukotriene B4 (LTB4), and Interleukin β4 (ILβ4) levels, indicated a significant reduction in inflammatory biomarkers in treated rats.

Additionally, these treatments exhibited improved histopathologic profiles compared to the positive control group. Boswellia oil and its Nano sponge formulation O1 and Dexa salt Nano sponge formulation D4 demonstrated promising therapeutic effects in managing both upper and lower respiratory allergic conditions. These findings suggest the potential clinical benefits of utilizing these formulations for treating respiratory allergies.

Acknowledgements We would like to express our great thanks and appreciation to in house project unit of National Research Centre, Dokki, Egypt for providing facilities for this work project under title: "Pharmacological investigation and Metabolomics study of promising anti-inflammatory herbal oils loaded in a polymeric nano-composite drug delivery system targeting Dermatitis and Upper Respiratory Allergy in rats" no. 12060132. We would like also to express our deep gratitude and grateful thanks to Prof. Dr Hab. Piotr Kachlicki; Head of Metabolomics team at Institute of Plant Genetics PAS Poznan, for his support and assistance for using UPLC/HRMS.

Author contributions Sally Abou Taleb: Conceptualization, Methodology, Investigation, Data curation. Bassant MM Ibrahim: Conceptualization, Methodology, Investigation, Data curation, Writing—original draft. Mona A. Mohammed: Conceptualization, Methodology, Investigation, Data curation, Writing—original draft. Noha Nazeeh Yassen: Methodology, Investigation, Formal analysis. Alyaa Farouk Hussein: Methodology, Investigation, Formal analysis. Shaimaa Ali Gad: Methodology, Investigation, Formal analysis. Asmaa Badawy Darwish: Conceptualization, Methodology, Investigation, Formal analysis, Data curation, Writing—original draft, review & editing.

Funding Open access funding provided by The Science, Technology & Innovation Funding Authority (STDF) in cooperation with The Egyptian Knowledge Bank (EKB).

Data availability All data generated or analyzed during this study are included in this published article.

Declarations

Competing interests All authors (S.A. Taleb, B.M.M. Ibrahim, M.A. Mohammed, N.N. Yassen, A.F. Hessin, S.A. Gad, and A.B. Darwish) report no conflict of interest.

Statement of human and animal rights The animal studies were performed after receiving approval of the Institutional Animal Care and Use Committee (IACUC) in ### University (IACUC approval No. ##-##-###).

References

Abou Taleb S, Darwish AB, Abood A, Mohamed AM (2019) Investigation of a new horizon antifungal activity with enhancing the antimicrobial efficacy of ciprofloxacin and its binary mixture via their encapsulation in nanoassemblies: in vitro and in vivo evaluation. Drug Dev Res

Abou Taleb S, Moatasim Y, GabAllah M, Asfour MH (2022) Quercitrin loaded cyclodextrin based nanosponge as a promising approach for management of lung cancer and COVID-19. J Drug Deliv Sci Technol 77:103921

Ahmed MM, Fatima F, Anwer MK, Ibnouf EO, Kalam MA, Alshamsan A, Aldawsari MF, Alalaiwe A, Ansari MJ (2021) Formulation and in vitro evaluation of topical nanosponge-based gel containing butenafine for the treatment of fungal skin infection. Saudi Pharm J 29(5):467–477

Al Amri A, Jesil A, Salim A, Saravanan A (2019) Extraction of essential oil from Frankincense using steam distillation. Int J Trend Res Dev 6(1):87–89

Allenova A, Darlenski R (2023) The hen and the egg question in atopic dermatitis: allergy or eczema comes first. Asthma Res Pract 9(1):1–4

Almutairy BK, Alshetaili A, Alali AS, Ahmed MM, Anwer MK, Aboudzadeh MA (2021) Design of olmesartan medoxomil-loaded nanosponges for hypertension and lung cancer treatments. Polymers 13(14):2272

Al-Owaidi MF, Alkhafaji SL, Mahood AM (2021) Quantitative determination of dexamethasone sodium phosphate in bulk and pharmaceuticals at suitable pH values using the spectrophotometric method. J Adv Pharm Technol Res 12(4):378–383

Ammar NM, Hassan HA, Mohammed MA, Serag A, Abd El-Alim SH, Elmotasem H, El Raey M, El Gendy AN, Sobeh M, Abdel-Hamid A-HZ (2021) Metabolomic profiling to reveal the therapeutic potency of *Posidonia oceanica* nanoparticles in diabetic rats. RSC Adv 11(14):8398–8410

Ammon HP, Safayhi H, Mack T, Sabieraj J (1993) Mechanism of antiinflammatory actions of curcumine and boswellic acids. J Ethnopharmacol 38(2–3):113–119

Ansari KA, Vavia PR, Trotta F, Cavalli R (2011a) Cyclodextrin-based nanosponges for delivery of resveratrol: in vitro characterisation, stability, cytotoxicity and permeation study. AAPS PharmSciTech 12(1):279–286

Ansari KA, Torne SJ, Vavia PR, Trotta F, Cavalli R (2011b) Paclitaxel loaded nanosponges: in-vitro characterization and cytotoxicity study on MCF-7 cell line culture. Curr Drug Deliv 8(2):194–202

Asahara M, Ito N, Hoshino Y, Sasaki T, Yokomizo T, Nakamura M, Shimizu T, Yamada Y (2022) Role of leukotriene B4 (LTB4)-LTB4 receptor 1 signaling in post-incisional nociceptive sensitization and local inflammation in mice. PLoS ONE 17(10):e0276135

Ayub MA, Hanif MA, Blanchfield J, Zubair M, Abid MA, Saleh MT (2022) Chemical composition and antimicrobial activity of Boswellia serrata oleo-gum-resin essential oil extracted by superheated steam. Nat Prod Res 1–6

Ayub MA, Hanif MA, Blanchfield J, Zubair M, Abid MA, Saleh MT (2023) Chemical composition and antimicrobial activity of *Boswellia serrata* oleo-gum-resin essential oil extracted by superheated steam. Nat Prod Res 37(14):2451–2456

Basha M, Abd El-Alim SH, Kassem AA, El Awdan S, Awad G (2015) Benzocaine loaded solid lipid nanoparticles: formulation design, in vitro and in vivo evaluation of local anesthetic effect. Curr Drug Deliv 12(6):680–692

Bianco A, Whiteman SC, Sethi SK, Allen JT, Knight RA, Spiteri MA (2000) Expression of intercellular adhesion molecule-1 (ICAM-1) in nasal epithelial cells of atopic subjects: a mechanism for increased rhinovirus infection? Clin Exp Immunol 121(2):339–345

Bocsan IC, Muntean IA, Miron N, Pintea I, Dobrican CT, Ureche C, Buzoianu AD, Deleanu D (2021) Are markers of allergic inflammation in grass pollen allergy influenced by H1 antihistamines? J Clin Med 11(1):113

Borotová P, Čmiková N, Galovičová L, Vukovic NL, Vukic MD, Tvrdá E, Kowalczewski PŁ, Kluz MI, Puchalski C, Schwarzová M (2023) Antioxidant, antimicrobial, and anti-insect properties of boswellia carterii essential oil for food preservation improvement. Horticulturae 9(3):333

Capozza K, Funk M, Hering M, Lang J, Merhand S, Manion R, Orevillo K, Picozza M, Proctor A, Schwennesen T (2023) Patients' and caregivers' experiences with atopic dermatitis-related burden, medical care, and treatments in 8 countries. J Allergy Clin Immunol 11(1):264–273

DeCarlo A, Ali S, Ceroni M (2020) Ecological and economic sustainability of non-timber forest products in post-conflict recovery: a case study of the Frankincense (*Boswellia* spp.) resin harvesting in Somaliland (Somalia). Sustainability 12(9):3578

Drury R, Wallington E (1980) Carleton's histological technique, 5th edn. Churchill Livingstone, New York

Dubey P, Sharma H, Shah S, Tyagi C, Chandekar A, Jadon R (2017) Formulations and evaluation of Cyclodextrin complexed Ceadroxil loaded nanosponges. Int J Drug Deliv 9:84

Gidwani B, Vyas A (2015) Inclusion complexes of bendamustine with β-CD, HP-β-CD and Epi-β-CD: in-vitro and in-vivo evaluation. Drug Dev Ind Pharm 41(12):1978–1988

Girigoswami A, Girigoswami K (2022) Versatile applications of nanosponges in biomedical Field: a glimpse on SARS-CoV-2 management. Bionanoscience 12(3):1018–1031

Guenther E (1952) The essential oils, vol 5

Hamed MA, Mohammed MA, Aboul Naser AF, Matloub AA, Fayed DB, Ali SA, Khalil WK (2019) Optimization of curcuminoids extraction for evaluation against Parkinson's disease in rats. J Biol Active Prod Nat 9(5):335–351

Han S, Liu J, Wang XS, Zhang Y, Luo Y-F (2020) Solubility enhancement of myricetin by inclusion complexation with heptakis-O-(2-hydroxypropyl)-β-cyclodextrin: a joint experimental and theoretical study. Int J Mol Sci 21:766

Huang K, Chen Y, Liang K, Xu X, Jiang J, Liu M, Zhou F (2022) Review of the chemical composition, pharmacological effects, pharmacokinetics, and quality control of *Boswellia carterii*. Evid Based Complement Altern Med 2022:6627104

Hussain H, Al-Harrasi A, Al-Rawahi A, Hussain J (2013) Chemistry and biology of essential oils of genus boswellia. Evid-Based Complement Altern Med

Kılıçarslan M, Baykara T (2003) The effect of the drug/polymer ratio on the properties of the verapamil HCl loaded microspheres. Int J Pharm 252(1–2):99–109

Kinsella JE (1966) Metabolic patterns of the fatty acids of *Periplanteta americana* (L.) during its embryonic development. Can J Biochem 44(2):247–258

Koeberle A, Henkel A, Verhoff M, Tausch L, König S, Fischer D, Kather N, Seitz S, Paul M, Jauch J, Werz O (2018) Triterpene acids from frankincense and semi-synthetic derivatives that inhibit 5-lipoxygenase and cathepsin G. Molecules 23(2):506

Kumar S, Pooja TF, Rao R (2018) Encapsulation of babchi oil in cyclodextrin-based nanosponges: physicochemical characterization, photodegradation, and in vitro cytotoxicity studies. Pharmaceutics 10:169

Kumar S, Prasad M, Rao R (2021) Topical delivery of clobetasol propionate loaded nanosponge hydrogel for effective treatment of psoriasis: formulation, physicochemical characterization, antipsoriatic potential and biochemical estimation. Mater Sci Eng C 119:111605

Lindler BN, Long KE, Taylor NA, Lei W (2020) Use of herbal medications for treatment of osteoarthritis and rheumatoid arthritis. Medicines 7(11):67

Lokhande AB, Mishra S, Kulkarni RD, Naik JB (2013) Preparation and characterization of repaglinide loaded ethylcellulose nanoparticles by solvent diffusion technique using high pressure homogenizer. J Pharm Res 7(5):421–426

Long J, Nand A, Bunt C, Seyfoddin A (2019) Controlled release of dexamethasone from poly(vinyl alcohol) hydrogel. Pharm Dev Technol 24:1–29

Mahalingam S, Thomas P, Karuppasamy V, Kulandaivel J, Geraldine P (2017) Synthesis and characterization of chrysin-loaded β-cyclodextrin-based nanosponges to enhance in-vitro solubility, photostability, drug release, antioxidant effects and antitumorous efficacy. J Nanosci Nanotechnol 17:8742–8751

Mazyed E, Zakaria S (2019) Enhancement of dissolution characteristics of clopidogrel bisulphate by proniosomes. Int J Appl Pharm 11:77–85

Mehta M, Dureja H, Garg M (2016) Development and optimization of boswellic acid-loaded proniosomal gel. Drug Deliv 23:1–10

Mikhaeil BR, Maatooq GT, Badria FA, Amer MM (2003) Chemistry and immunomodulatory activity of frankincense oil. Zeitschrift Für Naturforschung C 58(3–4):230–238

Mohammed MA (2023) Fighting cytokine storm and immunomodulatory deficiency: by using natural products therapy up to now. Front Pharmacol 14:1111329

Mohammed MA, El-Gengaihi SE, Enein AMA, Hassan EM, Ahmed OK, Asker MS (2016) Chemical constituents and antimicrobial activity of different Annona species cultivated in Egypt. J Chem Pharm Res 8:261–271

Mohammed MA, Attia HN, El-Gengaihi SE, Maklad YA, Ahmed KA, Kachlicki P (2021) Comprehensive metabolomic, lipidomic and pathological profiles of baobab (*Adansonia digitata*) fruit pulp extracts in diabetic rats. J Pharm Biomed Anal 201:114139

Mohammed MA, Hamed MA, El-Gengaihi SE, Enein AMA, Kachlicki P, Hassan EM (2022a) Profiling of secondary metabolites and DNA typing of three different Annona cultivars grown in Egypt. Metabolomics 18(7):49

Mohammed MA, Ibrahim BM, Abdel-Latif Y, Hassan AH, El Raey MA, Hassan EM, El-Gengaihi SE (2022b) Pharmacological and metabolomic profiles of *Musa acuminata* wastes as a new potential source of anti-ulcerative colitis agents. Sci Rep 12(1):1–24

Muqtader M, Fatima F, Anwer MK, Ibnouf E, Abul Kalam M, Alshamsan A, Aldawsari M, Alalaiwe A, Ansari M (2021) Formulation and in vitro evaluation of topical nanosponge-based gel containing butenafine for the treatment of fungal skin infection. Saudi Pharm J 29:467–477

Ni X, Suhail MM, Yang Q, Cao A, Fung K-M, Postier RG, Woolley C, Young G, Zhang J, Lin H-K (2012) Frankincense essential oil prepared from hydrodistillation of Boswellia sacra gum resins induces human pancreatic cancer cell death in cultures and in a xenograft murine model. BMC Complement Altern Med 12(1):1–14

Nikolić V, Stanković M, Nikolić L, Nikolić G, Ilić-Stojanović S, Popsavin M, Zlatković S, Kundaković T (2013) Inclusion complexes with cyclodextrin and usnic acid. J Incl Phenom Macrocycl Chem 76(1–2):173–182

Oliver SG, Winson MK, Kell DB, Baganz F (1998) Systematic functional analysis of the yeast genome. Trends Biotechnol 16(9):373–378

Olteanu AA, Aramă C-C, Radu C, Mihăescu C, Monciu C-M (2014) Effect of β-cyclodextrins based nanosponges on the solubility of lipophilic pharmacological active substances (repaglinide). J Incl Phenom Macrocycl Chem 80(1):17–24

Omar SM, Ibrahim F, Ismail A (2020) Formulation and evaluation of cyclodextrin-based nanosponges of griseofulvin as pediatric oral liquid dosage form for enhancing bioavailability and masking bitter taste. Saudi Pharm J 28(3):349–361

Osmani RAM, Kulkarni PK, Gowda V, Hani U, Gupta VK, Prerana M, Saha C (2018) Cyclodextrin-based nanosponges in drug delivery and cancer therapeutics: new perspectives for old problems. In: Applications of nanocomposite materials in drug delivery. Elsevier, Amsterdam, pp 97–147

Paczkowska-Walendowska M, Rosiak N, Tykarska E, Michalska K, Plazinska A, Plazinski W, Szymanowska-Powałowska D, Cielecka-Piontek J (2020) Tedizolid-cyclodextrin system as delayed-release drug delivery with antibacterial activity. Int J Mol Sci 22:115

Patel S, Rajput S (2009) Enhancement of oral bioavailability of cilostazol by forming its inclusion complexes. AAPS PharmSciTech 10:660–669

Peppas NA, Sahlin JJ (1989) A simple equation for the description of solute release. III. Coupling of diffusion and relaxation. Int J Pharm 57(2):169–172

Qnouch A, Solarczyk V, Verin J, Tourrel G, Stahl P, Danède F, Willart J, Lemesre P-E, Vincent C, Siepmann J, Siepmann F (2021) Dexamethasone-loaded cochlear implants: how to provide a desired "burst release." Int J Pharm X 3:100088

Rainsford KD (2007) Anti-inflammatory drugs in the 21st century. Subcell Biochem 42:3–27

Rhimi W, Mohammed MA, Zarea AAK, Greco G, Tempesta M, Otranto D, Cafarchia C (2022) Antifungal, antioxidant and antibiofilm activities of essential oils of Cymbopogon spp. Antibiotics 11(6):829

Rodrigues LB, Leite HF, Yoshida MI, Saliba JB, Cunha AS Jr, Faraco AA (2009) In vitro release and characterization of chitosan films as dexamethasone carrier. Int J Pharm 368(1–2):1–6

Schimmer B, Parker K (1996) Hormônio adrenocorticotrófico; esteróides adrenocorticais e seus análogos sintéticos; inibidores da síntese e das ações dos hormônios adrenocorticais. Goodman & Gilman's: as bases farmacológicas da terapêutica. 9a ed. Rio de Janeiro. McGraw-Hill, pp 1082–1102

Selvamuthukumar S, Anandam S, Krishnamoorthy K, Rajappan M (2012) Nanosponges: a novel class of drug delivery system-review. J Pharm Pharm Sci 15(1):103–111

Shankar G, Agrawal Y (2015) Formulation and evaluation of β-cyclodextrin based nanosponges of a poorly water soluble drug. J Chem Pharm Res 7(4):595–604

Sharma R, Walker R, Pathak K (2011) Evaluation of the kinetics and mechanism of drug release from econazole nitrate nanosponge loaded carbapol hydrogel. Indian J Pharm Educ Res 45:25–31

Shrestha S, Bhattacharya S (2020) Versatile use of nanosponge in the pharmaceutical arena: a mini-review. Recent Pat Nanotechnol 14:351–359

Siemoneit U, Pergola C, Jazzar B, Northoff H, Skarke C, Jauch J, Werz O (2009) On the interference of boswellic acids with 5-lipoxygenase: mechanistic studies in vitro and pharmacological relevance. Eur J Pharmacol 606(1–3):246–254

Sorg DA, Buckner B (1964) A simple method of obtaining venous blood from small laboratory animals. Proc Soc Exp Biol Med 115:1131–1132

Sunil K, Pooja D, Rekha R (2019) Cyclodextrin nanosponges: a promising approach for modulating drug delivery. In: Selcan K (ed) Colloid sci pharm nanotechnol, ch. 6. IntechOpen, Rijeka

Swaminathan S, Pastero L, Serpe L, Trotta F, Vavia P, Aquilano D, Trotta M, Zara G, Cavalli R (2009) Cyclodextrin-based nanosponges encapsulating camptothecin: physicochemical characterization, stability and cytotoxicity. Eur J Pharm Biopharm 74:193–201

Swaminathan S, Pastero L, Serpe L, Trotta F, Vavia P, Aquilano D, Trotta M, Zara G, Cavalli R (2010) Cyclodextrin-based nanosponges encapsulating camptothecin: physicochemical characterization, stability and cytotoxicity. Eur J Pharm Biopharm 74(2):193–201

Tham EH, Leung DY (2019) Mechanisms by which atopic dermatitis predisposes to food allergy and the atopic march. Allergy Asthma Immunol Res 11(1):4–15

Trotta F, Cavalli R, Tumiatti W, Zerbinati O, Roggero C, Vallero R (2008) Ultrasound-assisted synthesis of cyclodextrin-based nanosponges, Google Patents

Trotta F, Zanetti M, Cavalli R (2012) Cyclodextrin-based nanosponges as drug carriers. Beilstein J Org Chem 8:2091–2099

Utzeri G, Matias PMC, Murtinho D, Valente AJM (2022) Cyclodextrin-based nanosponges: overview and opportunities. Front Chem 10:859406

Vestbo J, Sørensen T, Lange P, Brix A, Torre P, Viskum K (1999) Long-term effect of inhaled budesonide in mild and moderate chronic obstructive pulmonary disease: a randomised controlled trial. Lancet 353(9167):1819–1823

Vyas A, Saraf S, Saraf PS (2008a) Cyclodextrin based novel drug delivery systems. J Incl Phenom Macrocycl Chem 62:23–42

Vyas A, Saraf S, Saraf S (2008b) Cyclodextrin based novel drug delivery systems. J Incl Phenom Macrocycl Chem 62(1):23–42

Wise R, Connett J, Weinmann G, Scanlon P, Skeans M (2000) Effect of inhaled triamcinolone on the decline in pulmonary function in chronic obstructive pulmonary disease. N Engl J Med 343(26):1902–1909

Yaşayan G, Şatıroğlu Sert B, Tatar E, Küçükgüzel İ (2020) Fabrication and characterisation studies of cyclodextrin-based nanosponges for sulfamethoxazole delivery. J Incl Phenom Macrocycl Chem 97(3):175–186

Yassin NA, El-Shenawy SM, Mahdy KA, Gouda NA, Marrie AE-FH, Farrag ARH, Ibrahim BM (2013) Effect of *Boswellia serrata* on Alzheimer′s disease induced in rats. J Arab Soc Med Res 8(1):1–11

Younis MM, Fadel NAE-F, Darwish AB, Mohsen AM (2023) Nanospanlastics as a novel approach for improving the oral delivery of resveratrol in lipopolysaccharide-induced endotoxicity in mice. J Pharm Innov

Zidan MF, Ibrahim HM, Afouna MI, Ibrahim EA (2018) In vitro and in vivo evaluation of cyclodextrin-based nanosponges for enhancing oral bioavailability of atorvastatin calcium. Drug Dev Ind Pharm 44(8):1243–1253